Complex Hydrides for Hydrogen Storage

Shin-ichi Orimo,[†] Yuko Nakamori,[†] Jennifer R. Eliseo,[‡] Andreas Züttel,[§] and Craig M. Jensen*[,‡,||]

Institute for Materials Research, Tohoku University, Sendai 980-8577, Japan, Hawaii Hydrogen Carriers, LLC, Honolulu, Hawaii 96813, Department of Mobility, Environment, and Energy, EMPA Materials Sciences and Technology, 8600 Dübendorf, Switzerland, and Department of Chemistry, University of Hawaii, Honolulu, Hawaii 96822

Received June 7, 2007

Contents

* Corresponding e-mail: jensen@hawaii.edu.
[†] Tohoku University.
[‡] Hawaii Hydrogen Carriers, LLC.
[§] EMPA Materials Sciences and Technology.
[||] University of Hawaii.

1. Introduction

A major obstacle to the conversion of the world to a "hydrogen economy" is the problem of onboard hydrogen storage. High-pressure and cryogenic hydrogen storage systems are impractical for vehicular applications due to safety concerns and volumetric constraints. This has prompted an extensive effort to develop solid hydrogen storage systems for vehicular application. Metal hydrides,[1,2] activated charcoal,[3,4] and advanced carbons[5−7] have been investigated as hydrogen carriers. Unfortunately, despite decades of extensive effort, no material has been found which has the combination of a high gravimetric hydrogen density, adequate hydrogen-dissociation energetics, reliability, and low cost required for commercial vehicular application.[8−10]

Group I and II salts of $[AlH_4]^-$, $[NH_2]^-$, and $[BH_4]^-$ (alanates, amides, and borohydrides) have recently received considerable attention as potential hydrogen storage materials. All of these materials are currently referred to as "complex hydrides", although only the alanates contain anionic metal complexes. However, like the alanates, amides and borohydrides are saline materials in which hydrogen is covalently bonded to central atoms in "complex" anions (in contrast to interstitial hydrides). [In this review, "amides" refers to mixtures of amides and metal hydrides that undergo reversible dehydrogenation, as opposed to amides alone. Although it is technically imcomplete, the term "amide" has been generally adopted for this group of hydrogen storage materials by researchers working in the area of complex hydrides. Accordingly, the commonly employed "amide" label is used throughout the text.] These materials have high hydrogen gravimetric densities (Table 1) and are, in some cases, commercially available. Thus, a priori, they would seem to be viable candidates for application as practical, onboard hydrogen storage materials. Many of these "complex hydrides" have, in fact, been utilized in "one-pass" hydrogen storage systems in which hydrogen is evolved from the hydride upon contact with water. However, the hydrolysis reactions are highly irreversible and could not serve as the basis for rechargeable hydrogen storage systems. The thermodynamics of the direct, reversible dehydrogenation of some complex hydrides lie within the limits that are required for a practical, onboard hydrogen carrier. All of these materials are, however, plagued by high kinetics barriers to dehydrogenation and/or rehydrogenation in the solid state. Traditionally, it was thought that it would be impossible to reduce the barrier heights to an extent that would give

10.1021/cr0501846 CCC: $65.00
Published on Web 09/12/2007

Shin-ichi Orimo was born in Hiroshima, Japan, in 1966. He was a JSPS (Japan Society for the Promotion of Science) Research Fellow (1993–1995) and received his Ph.D. degree from Hiroshima University in 1995, for his work on the Mg-, Zr-, and Y-based metal hydrides. He was a research associate at Hiroshima University (1995–2002) and also a guest researcher at the Max-Planck Institute for Metal Research and was awarded a Alexander von Humboldt Fellowship and an MEXT (Ministry of Education, Culture, Sports, Science and Technology) Fellowship (1998–1999). In 2002, he moved to the Institute for Materials Research, Tohoku University, to start up a new laboratory on hydride research with Yuko Nakamori. He has been awarded the Best Young Researcher Award and the Murakami Memorial Encouraged Research Award (The Japan Institute of Metals), the Encouraged Research Award (Materials Science Foundation, Japan), the Promoted Research Award (Japan Magnesium Association), and the Intelligent Cosmos Prize, (Intelligent Cosmos Foundation). His laboratory is currently focusing on new complex, alloy, and perovskite hydrides composed of lightweight metals and specific nanostructures, aiming at developing materials for hydrogen storage, neutron shielding, secondary batteries, and ionic conductors.

Yuko Nakamori was born in Hiroshima, Japan, in 1973. She received her Ph.D. degree in 2002 at the Faculty of Integrated Arts and Sciences, Hiroshima University, for her work on magnetic properties of rare-earth intermetallic compounds. She moved to the Institute for Materials Research, Tohoku University, in 2002 as a research associate to work with Shin-ichi Orimo on complex hydrides, specifically for development of advanced hydrogen storage materials. She was awarded the Promoted Research Award for Young Scientists from the Materials Research Society of Japan (MRS-J) and the Japan Institute of Metals in 2004 and 2005, respectively. Her research interests are fundamental, physical, and chemical properties of lightweight hydrides, and hydrogen storage applications using electromagnetic fields.

reaction rates that even approached those that would be required for vehicular applications. Thus, until recently, complex hydrides were not considered as candidates for application as rechargeable hydrogen carriers. This situation was changed by Bogdanović and Schwickardi. Their pioneering studies demonstrated that, upon doping with selected titanium compounds, the dehydriding of anionic aluminum

Jennifer R. Eliseo is originally from Burnt Hills, New York. She completed her undergraduate work at Union College (Schenectady, New York), where she was the recipient of the William H. Wright Chemistry Scholarship. Jennifer recently graduated from the University of Hawaii with a M.S. in Chemistry. Currently, she works as chief technical writer at Hawaii Hydrogen Carriers, LLC. She plans to pursue a career in advanced material science.

Andreas Züttel was born in Bern, Switzerland, in 1963. He received his Dr. rer. nat. from the Science Faculty at the University of Fribourg in 1993, and he was a Post Doc with AT&T Bell Labs in Murray Hill, New Jersey, U.S.A., in 1994. He became Head of the Metalhydride and Energy Storage Group (in 1996) and then Lecturer at the Physics Department of the University of Fribourg (in 1997). In 2001, he became Vice President of the Swiss Hydrogen Association "Hydropole", a Member of the Scientific Advisory Board of IMRA EUROPE, and a Member of the Technical Advisory Committee of HERA, and in 2003, he became an External Professor at the Vrije Universiteit van Amsterdam, Netherlands. In 2004, he completed his Habilitation in Experimental Physics at the Science Faculty of the University of Fribourg, Switzerland, and became Vice-President of the Swiss Physical Society (SPS) and President of the Swiss Hydrogen Association "HYDROPOLE". He moved to the Swiss National Institute for Materials Research and Testing, Empa, in 2006, as Head of the section "Hydrogen & Energy". He is currently a Prof. tit. in the Physics Department of the University of Fribourg.

hydrides could be kinetically enhanced and rendered reversible under moderate conditions in the solid state.[11] This breakthrough has led to a worldwide effort to develop doped alanates as practical hydrogen storage materials that was quickly expanded to include amides and borohydrides.

Any effort to develop complex hydrides as practical hydrogen storage materials requires knowledge of their atomic structure and the thermodynamics of their fundamental dehydrogenation and rehydrogenation reaction chemistry. This review provides a summary of information and an overview of the progress that has been made toward the utilization of alantes, amides, and borohydrides as onboard

Craig M. Jensen is a Professor of Chemistry at the University of Hawaii. He was born and raised in Wenatchee, Washington, U.S.A. His undergraduate education began at the University of Washington and was completed, after a sabbatical in the Aleutian Islands, at the University of California at Santa Barbara, and he obtained his Ph.D. at the University of California at Los Angeles under the supervision of Professor H. D. Kaesz. Following a postdoctoral appointment at the University of California at San Diego, he joined the faculty at UH in 1986. He is an inorganic chemist with broad experience in catalyst development and the synthesis and characterization of novel inorganic and organometallic materials. In recognition of his work with hydrogen storage materials, he was awarded the DOE Hydrogen Program's "1999 Research Success Story" award and the DOE EERE "R&D" award in 2004. He recently served as a co-chairman of the 2006 International Symposium on Metal–Hydrogen Systems and co-chair of the 2007 Hydrogen–Metal Systems Gordon Research Conference. He is president and founder of Hawaii Hydrogen Carriers, LLC.

hydrogen carriers. We have focused on materials with high practical potential and have excluded those with properties that clearly preclude practicality, such as the high toxicity of beryllium based compounds.

2. Alanates

2.1. Synthesis

One attractive feature of alanates is that lithium and sodium salts are readily available commercially. Magnesium alanate can be readily prepared with sodium alanate and magnesium hydride via a metathesis reaction.[12] The mixed metal alanate, Na_2LiAlH_6, is prepared through ball milling of sodium hydride, lithium hydride, and sodium alanate.[13] Potassium alanate can be prepared by the direct synthesis of potassium hydride and aluminum under high temperature and pressure.[14]

2.2. Atomic Structure

2.2.1. $NaAlH_4$

Lauher et al.[15] determined the atomic structure of $NaAlH_4$ through a single-crystal X-ray diffraction study in 1979. Refinement of their data in space group $I4_1/a$ showed the compound to consist of isolated $[AlH_4]^-$ tetrahedra in which the Na atoms are surrounded by eight $[AlH_4]^-$ tetrahedra in a distorted square antiprismatic geometry. Their results gave an Al−H bond length of 1.532(0.07) Å. These findings were significantly shorter than the Al−H bond distances that were previously determined from a single-crystal X-ray study of $LiAlH_4$[16] (average value of 1.548(0.17) Å). Bel'skii et al.[17] noted that this was inconsistent with the implications of the infrared spectra of the compounds, as the Al−H stretching frequency of $NaAlH_4$ is observed at a lower frequency than that of $LiAlH_4$ (1680 and 1710 cm^{-1}, respectively). A second single crystal study generated data that converged to give an Al−H distance of 1.61(0.04) Å[17] that was in agreement with the IR data. However, it was noted that full resolution of the issue of the Al−H bond distance required neutron diffraction data, as X-ray diffraction data tends to give erroneously short metal−hydrogen distances and very large uncertainties in the determination of hydrogen coordinates.

The structure of $NaAlD_4$ has been determined by powder neutron diffraction data[18] at 8 and 295 K. Selected interatomic distances and bond angles are given in Table 2. The atomic structure was found to be made up of isolated $[AlD_4]^-$ tetrahedra surrounded by sodium atoms (Figure 1). The shortest Al−Al separations were 3.737(0.01) and 3.779(0.01) Å at 8 and 295 K, respectively. The two unique Na−D bond distances were nearly equal, 2.403(0.02) and 2.405(0.02) Å at 8 K and 2.431(0.02) and 2.439(0.02) Å at 295 K. The Al−D distances were found to be 1.626(0.02) and 1.627(0.02) Å at 8 and 295 K, respectively. Previously, X-ray data by Bel'skii et al.[17] reported a shorter and much more uncertain Al−D distance of 1.61(0.04) Å. Upon cooling from 295 to 8 K, the Al−D distances showed no significant change. The two unique D−Al−D bond angles in the $[AlD_4]^-$ tetrahedron were reported to be 107.32° and 113.86° at 295 K.

2.2.2. $LiAlH_4$

The crystal structure of $LiAlH_4$ was originally determined by Sklar and Post[16] through an X-ray diffraction study. Hauback et al.[19] carried out a more detailed atomic structure

Table 1. Material Properties of Complex Hydrides[254]

material	CAS no.	density (g/mol)	density (g/cm^3)	hydrogen (wt %)	hydrogen (kg/m^3)	T_m[a] (°C)	ΔH_f° (kJ/mol)
$LiAlH_4$	16853-85-3	37.95	0.917	10.54		190[d]	−119
$NaAlH_4$	13770-96-2	54.00	1.28	7.41		178	−113
$KAlH_4$		70.11		5.71	53.2		
$Mg(AlH_4)_2$	17300-62-8	86.33		9.27	72.3		
$Ca(AlH_4)_2$	16941-10-9	102.10		7.84	70.4	>230[d]	
$LiNH_2$	7782-89-0	22.96	1.18	8.78	103.6	372−400	−179.6
$NaNH_2$	7782-92-5	39.01	1.39	5.15	71.9	210	−123.8
KNH_2	17242-52-3	55.12	1.62	3.66	59.3	338	−128.9
$Mg(NH_2)_2$	7803-54-5	56.37	1.39	7.15	99.4	360	
$Ca(NH_2)_2$	23321-74-6	72.13	1.74	5.59	97.3		−383.4
$LiBH_4$	16949-15-8	21.78	0.66	18.36	122.5	268	−194
$NaBH_4$	16940-66-2	37.83	1.07	10.57	113.1	505	−191
KBH_4	13762-51-1	53.94	1.17	7.42	87.1	585	−229
$Mg(BH_4)_2$	16903-37-0	53.99	0.989	14.82	146.5	320[d]	
$Ca(BH_4)_2$	17068-95-0	69.76		11.47		260[d]	
$Al(BH_4)_3$	16962-07-5	71.51	0.7866	16.78	132	−64.5[d] 44.5[b]	

[a] d and b represent decomposition and boiling temperatures, respectively.

Table 2. Selected Interatomic Distances (Å) and Angles (deg) in Various Crystal Structures at 8 and 295 K

material/ref	atoms	295 K	8 K
$NaAlD_4$	Al−D (×4)	1.626(0.02)	1.627(0.02)
ref 18	Na−D (×4)	2.431(0.02)	2.403(0.02)
	(×4)	2.439(0.01)	2.405(0.02)
	Al−Na (×4)	3.544(0.01)	3.521(0.01)
	(×4)	3.779(0.01)	3.737(0.01)
	D−Al−D (×4)	107.32(1)	107.30(1)
	(×2)	113.86(1)	113.90(1)
$LiAlD_4$	Al−D1	1.605(0.06)	1.625(0.06)
ref 19	Al−D2	1.633(0.05)	1.621(0.05)
	Al−D3	1.623(0.05)	1.645(0.05)
	Al−D4	1.603(0.07)	1.596(0.06)
	Li−D1	1.920(0.08)	1.896(0.12)
	Li−D2	1.936(0.07)	1.932(0.09)
		1.978(0.08)	1.978(0.12)
	Li−D3	1.831(0.06)	1.841(0.09)
	Li−D4	1.909(0.08)	1.870(0.10)
	Li−Al	3.214(0.06)	3.200(0.09)
		3.234(0.05)	3.232(0.12)
		3.260(0.04)	3.265(0.11)
		3.328(0.06)	3.285(0.10)
		3.415(0.06)	3.401(0.12)
	D1−Al−D2	110.1(3)	109.0(3)
	D1−Al−D3	109.2(3)	108.2(3)
	D1−Al−D4	110.8(3)	111.0(3)
	D2−Al−D3	108.7(3)	108.9(3)
	D2−Al−D4	107.1(3)	108.4(4)
	D3−Al−D4	111.0(3)	111.3(3)
$KAlD_4$	Al−D1 (×1)	1.546(0.13)	1.589(0.07)
ref 20	Al−D2 (×1)	1.669(0.13)	1.659(0.07)
	Al−D3 (×2)	1.629(0.08)	1.638(0.04)
	K−D1 (×1)	2.596(0.14)	2.627(0.07)
	K−D2 (×1)	2.833(0.15)	2.772(0.08)
	K−D2 (×2)	3.182(0.06)	3.137(0.03)
	K−D3 (×2)	2.840(0.10)	2.753(0.06)
	K−D3 (×2)	2.883(0.11)	2.841(0.06)
	K−D3 (×2)	2.980(0.12)	2.955(0.06)
	D3−Al−D3	106.7(23)	106.39(12)
	D3−Al−D2	106.5(18)	107.39(10)
	D3−Al−D1	111.2(18)	111.05(9)
	D2−Al−D1	114.56(72)	113.3(4)
Na_3AlD_6	Al−D1	1.746	
ref 22	Al−D2	1.758	
	Al−D3	1.770	
	Na1−D1	2.268	
	Na1−D2	2.226	
	Na1−D3	2.261	
	Na2−D1	2.267	
		2.391	
	Na2−D2	2.307	
		2.669	
		2.699	
	Na2−D3	2.299	
		2.627	
		2.766	
	D1−Al−D2	88.9	
	D1−Al−D3	89.0	
	D2−Al−D3	89.4	
Li_3AlD_6	Al1−D1	1.754(0.04)	
ref 23	Al2−D2	1.734(0.04)	
	Li−D1	1.892(0.10)	
		2.009(0.12)	
		2.120(0.12)	
	Li−D2	1.948(0.08)	
		1.987(0.09)	
		2.051(0.14)	
	D1−Al1−D1	86.98(15)	
		93.02(15)	
		180.00(22)	
	D2−Al2−D2	87.36(13)	
		92.64(13)	
		180.00(22)	
Na_2LiAlD_6	Al−D	1.760(0.03)	
ref 25	Li−D	1.933(0.03)	
	D−Al−D	90.00(−), 180.00(−)	
$Mg(AlH_4)_2$	Al−H1	1.561(0.12)	1.606(0.10)
ref 21	Al−H2	1.672(0.04)	1.634(0.04)
	Mg−H2	1.833(0.07)	1.870(0.06)
	Mg−Al	3.459(0.01)	3.482(0.04)
	H1−Al−H2	110.1(3)	113.5(2)
	H2−Al−H2	108.79(15)	105.24(13)

[a] Estimated standard deviations are given in parentheses.

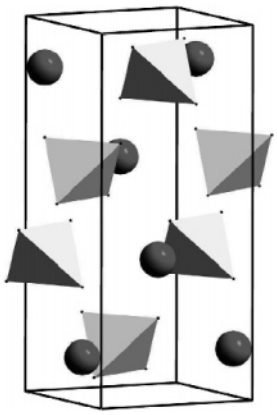

Figure 1. Crystal structure of $NaAlD_4$. The complex AlH_4^- anions are depicted as tetrahedra and the Na cations as black spheres.[18] Reprinted with permission from ref 18. Copyright 2003 Elsevier.

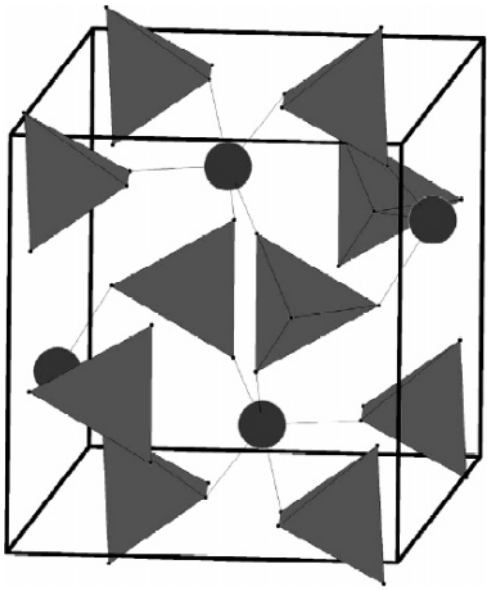

Figure 2. Crystal structure of $LiAlD_4$. The complex AlH_4^- anions are depicted as tetrahedra and the Li cations as black spheres.[19] Reprinted with permission from ref 19. Copyright 2002 Elsevier.

determination of $LiAlD_4$ based on combined powder neutron and X-ray diffraction studies. The compound crystallized in the space group $P2_1/c$. The atomic structure was found to consist of isolated $[AlD_4]^-$ tetrahedra surrounded by lithium atoms (Figure 2). Selected interatomic distances and bond angles are given in Table 2. The minimum Al−Al distance between tetrahedra was 3.754(0.01) Å at 295 K. The Al−D distances averaged 1.619(0.07) Å at 295 K, which are longer than the distances ranging from 1.516 to 1.578 Å that were deduced from the X-ray structure determination.[16] The D−Al−D angles of $LiAlD_4$ were found to vary by less than 1.5° from the angles of a perfect tetrahedron. The Li−D distances ranged from 1.831(0.06) to 1.978(0.08) Å at 295 K and from 1.841(0.09) to 1.978(0.12) Å at 8 K.

2.2.3. $KAlH_4$

The crystal structure of $KAlD_4$ has been determined by Hauback et al.[20] $KAlD_4$ has a $BaSO_4$-type structure with space group *Pnma*. The structure (Figure 3) consists of isolated $[AlD_4]^-$ tetrahedra in which potassium atoms are surrounded by seven of the tetrahedra (ten D atoms total). Selected interatomic distances and bond angles are given in Table 2. The average Al−D distance was 1.631 Å at 8 K

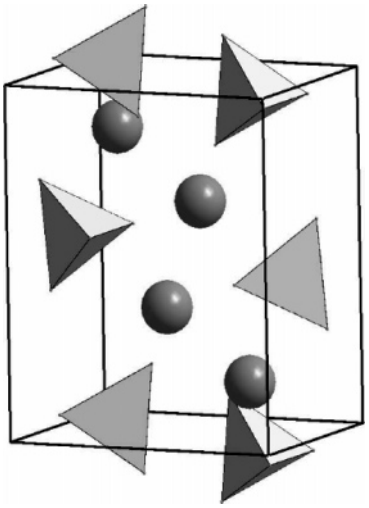

Figure 3. Crystal structure of $KAlD_4$. The complex AlH_4^- anions are depicted as tetrahedra and the K cations as black spheres.[20] Reprinted with permission from ref 20. Copyright 2005 Elsevier.

and 1.618 Å at 295 K. The minimum Al−Al distance between the tetrahedra was 4.052 Å at 295 K. Also, D−Al−D bond angles were close to ideal and ranged from 106.4 to 113.3° at 8 K and 106.2−114.6° at 295 K. In addition, the minimum K−D distance was 2.596 Å at 295 K (larger than the Na−D distance of $NaAlD_4$ and the Li−D distance of $LiAlD_4$).

It is noteworthy that variations in the crystal structures of $MAlH_4$ compounds (M = Li, Na, K) arise from the differences in the size of the alkali cations of Li^+, Na^+, and K^+, which result in coordination numbers of 5, 8, and 10, respectively.

2.2.4. $Mg(AlH_4)_2$

The structure of magnesium alanate was determined by Fossdal et al.[21] through a combination of X-ray and neutron diffraction. The space group was confirmed to be $P3m1$. The structure consists of a sheetlike arrangement consisting of $[AlH_4]^-$ tetrahedra surrounded by six Mg atoms in a distorted MgH_6 octahedral geometry (Figure 4). Selected interatomic distances and bond angles are shown in Table 2. The Al−H distances ranged from 1.606(0.10) to 1.634(0.04) Å at 8 K and from 156.1(0.12) to 167.2(0.04) pm at 295 K. These distances are in the same range as those found for lithium, sodium, and potassium alanate.

2.2.5. Na_3AlH_6 and Li_3AlH_6

In 2002, Rönnebro et al.[22] explored the perovskite-related structure of Na_3AlH_6. These studies determined the positions of the hydrogen atoms from neutron diffraction data of a deuterated sample. It was found that the best fit data was for the monoclinic space group $P2_1/n$. The structure was a distorted fcc structure of $[AlD_6]^{3-}$ units with sodium in all of the octahedral and tetrahedral sites. The complex anions were found to be distorted $[AlH_6]^{3-}$ octahedron. Selected interatomic distances and bond angles are reported in Table 2. The Al−D distances were 1.746, 1.758, and 1.770 Å, which are longer than the Al−D distances for $NaAlD_4$ (1.626(0.02) Å). The D−Al−D bond angles ranged from 88.9 to 89.4°. The Na−D distances ranged from 2.226 to 2.766 Å.

The structure of Li_3AlD_6 was determined by Brinks et al. through X-ray and neutron diffraction.[23] The space group

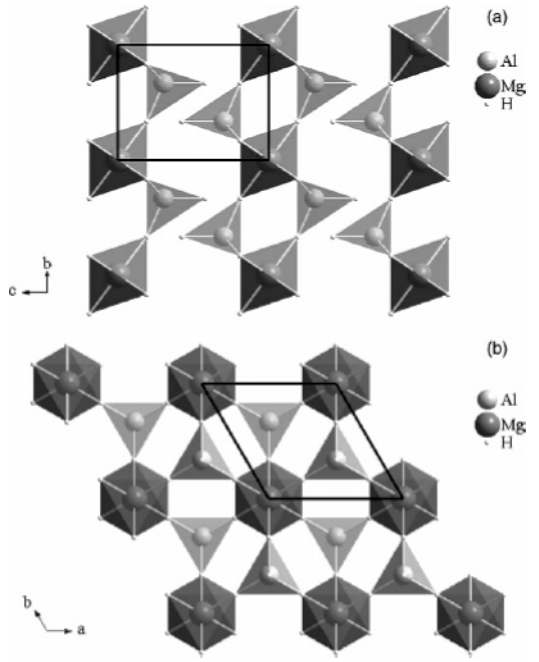

Figure 4. Crystal structure of $Mg(AlH_4)_2$. Views along (a) the *a*-axis and (b) the *c*-axis.[21] Reprinted with permission from ref 21. Copyright 2005 Elsevier.

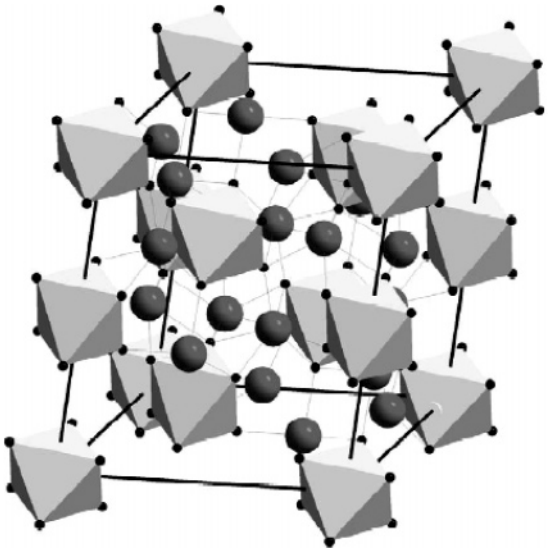

Figure 5. Crystal structure of Li_3AlD_6. The complex $[AlH_6]^{3-}$ anions are depicted as octahedra and the Li cations as spheres. Reprinted with permission from ref 23. Copyright 2003 Elsevier.

was found to be $R\bar{3}$, and the structure (Figure 5) consisted of isolated $[AlD_6]^{3-}$ octahedra connected by six-coordinated Li atoms (each Li atom is coordinated to two corners and two edges of the octahedral, six hydrogen atoms total). The structure is described as a distorted bcc of $[AlD_6]^{3-}$ units with half the tetrahedral sites filled with Li.[24] Selected interatomic distances and bond angles are given in Table 2. The Al−D distances were 1.734 and 1.754 Å, which are comparable to the 1.758 Å (average) found for the sodium analogue.[22] The D−Al−D bond angles were in the range from 86.98 to 93.02°. The Li−D distances ranged from 1.892 to 2.120 Å, and the shortest Al−Al distance was 4.757 Å.

It is important to note that Li has a coordination number of only 6 in Li_3AlD_6,while Na has coordination numbers of 6 and 8 in Na_3AlH_6.[22] This is due to the differences in the

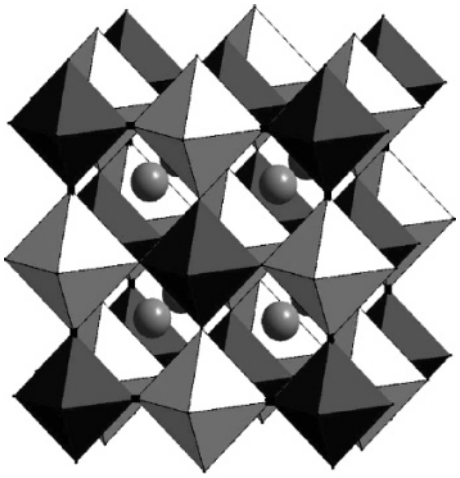

Figure 6. Crystal structure of Na_2LiAlD_6 at 22 °C showing alternating AlD_6 (dark) and LiD_6 (bright) octahedra in all directions with Na in interstitial 12-coordinated sites.[25] Reprinted with permission from ref 25. Copyright 2005 Elsevier.

size of the alkali metal ions.

2.2.6. Na_2LiAlH_6

The structure of Na_2LiAlD_6 (Figure 6) was determined by Brinks et al.[25] The structure was well defined in a cubic unit cell with a space group of $Fm\bar{3}m$. The compound had a perovskite-type structure best described as a distorted fcc of $[AlD_6]^{3-}$ units with Li in the octahedral sites and Na in the tetrahedral sites. Selected interatomic distances are given in Table 2. The Al−D bond distances were found to be 1.760-(0.03) Å. The Al−D bond distances of the $[AlD_6]^{3-}$ octahedra were significantly shorter in size than the octahedra of Li_3AlD_6 (average of 1.774 Å)[23] and longer than the octahedra of Na_3AlD_6 (1.756 Å).[22] The AlD_6 octahedra of Na_2LiAlD_6 are ideal, having equal Al−D distances and ideal angles. The shortest Al−Al distance was 5.222 Å.

2.3. Dehydrogenation and Rehydrogenation Reactions

2.3.1. Undoped Alanate

Dehydrogenation Reactions. Alkali metal alanates undergo dehydrogenation in the 200−300 °C temperature range (Li, 201 °C; Na, 265 °C; K, 290 °C) to give aluminum metal and the corresponding alkali metal hydrides (see eq 1).

$$NaAlH_4 \rightarrow NaH + Al + {}^3/_2H_2 \quad (1)$$

Further dehydrogenation of the binary metal hydrides occurs only at temperatures in excess of 400 °C. In 1952, Garner and Haycock[26] found that the dehydrogenation of $LiAlH_4$ in the 100−150 °C temperature range results in elimination of only 50% of the hydrogen content of the hydride rather than the 75% observed at 200 °C. They concluded that dehydrogenation to LiH and aluminum must be a two-step process involving an intermediate "$LiAlH_2$" phase. The dehydrogenation of $NaAlH_4$ was extensively studied by Ashby and Kobetz.[27] They found that controlled heating at 210−220 °C for 3 h evolved 3.7 wt % hydrogen to give Na_3AlH_6. This work established that the first step of the dehydrogenation proceeds according to eq 2 and that further elimination of hydrogen to give aluminum and NaH occurrs through a separate reaction (seen in eq 3) that takes place at ∼250 °C.

$$3NaAlH_4 \rightarrow Na_3AlH_6 + 2Al + 3H_2 \quad (2)$$

$$Na_3AlH_6 \rightarrow 3NaH + Al + {}^3/_2H_2 \quad (3)$$

The occurrence of these two distinct reactions during the dehydrogenation process has been verified in subsequent studies of the thermolysis of $LiAlH_4$, $NaAlH_4$, and $KAlH_4$ by a variety of techniques including differential thermal X-ray diffraction,[28] thermal gravimetric analysis,[29,30] hydrogen pressure−composition ($p-c$) isotherm (PCT) studies,[31,32] and, most recently, in situ X-ray diffraction study.[33]

The thermal dehydrogenation of $LiAlH_4$ was studied by Block and Gray in 1965 through differential scanning calorimetry.[34] This study confirmed the multistep dehydrogenation pathway and provided the first detailed information about the thermodynamic parameters of this process. They found that $LiAlH_4$ undergoes a phase transition at 160−177 °C before undergoing an initial dehydrogenation reaction to give Li_3AlH_6, as seen in eq 4 at 187−218 °C. This first dehydrogenation process was determined to be exothermic and with a ΔH of −10 kJ/(mol of H_2). Since the entropy of

$$LiAlH_4 \rightarrow {}^1/_3Li_3AlH_6 + {}^2/_3Al + H_2 \quad (4)$$

hydrogenation must be negative, this is a nonspontaneous process under all conditions. A second dehydrogenation reaction, seen in eq 5, was observed to occur at 228−282 °C. This reaction was found to be endothermic with a ΔH

$$Li_3AlH_6 \rightarrow 3LiH + Al + {}^3/_2H_2 \quad (5)$$

of 25 kJ/(mol of H_2). Finally, the dehydrogenation of LiH was observed in the 370−483 °C temperature range. The enthalpy of the dehydrogenation of $LiH_{(s)}$ has subsequently been determined to be 140 kJ/mol.[35]

The thermodynamics of the dehydrogenation of $NaAlH_4$ to NaH and Al was first studied by Dymova and Bakum in 1969 through differential thermal X-ray diffraction.[28] This was followed by more detailed thermal gravimetric and differential scanning calometric studies by Claudy et al.[36,37] The latter study revealed that, in addition to the chemical transformations seen in eqs 2 and 3, the thermal decomposition of the hydride also involves the melting of $NaAlH_4$ and the conversion of pseudocubic α-Na_3AlH_6 to face-centered cubic β-Na_3AlH_6. Consideration of the enthalpic values determined in these studies for the Na_3AlH_6 phase change (1.8 kJ/mol), the dehydrogenation of β-Na_3AlH_6 (13.8 kJ/mol), and the direct dehydrogenation of $NaAlH_4$ to NaH and Al (56.5 kJ/mol) allows the calculation of a ΔH of 40.9 kJ/mol for the solid-state dehydrogenation of $NaAlH_4$ to Na_3AlH_6. A similar value of ΔH for this process (36.0 kJ/mol) can be derived for the solid-state dehydrogenation by combining the heat of fusion of $NaAlH_4$ (23.2 kJ/mol) determined by Claudy et al. with the ΔH for the dehydrogenation of liquid $NaAlH_4$ to Na_3AlH_6 (12.8 kJ/mol).[32] PCT studies of sodium aluminum hydride were first carried out by Dymova et al.[32] The observation of two plateaus in these studies clearly confirmed the occurrence of two independent dehydrogenation reactions. At 210 °C, hydrogen plateau pressures of 15.4 and 2.1 MPa were found for the first and second reaction, respectively. The potential of solid $NaAlH_4$ as a practical onboard hydrogen storage material was obscured for many years because of the high kinetic barriers to the dehydrogenation reactions and their reverse. Also, pure sodium aluminum hydride melts at 183 °C. Since dehydro-

genation occurs at higher temperatures, only the unacceptably high plateau pressures associated with the much lower ΔH_{dehyd} of liquid $NaAlH_4$ could be observed.

The initial dehydrogenation of $KAlH_4$ to the hexahydride occurs at a much higher temperature (300 °C) than the analogous process for $NaAlH_4$. Morioka et al.[38] have pointed out that this might be the result of differing thermodynamic stabilities associated with the parent alanates, as the formation energies of KH and NaH are nearly equal (−56.3 and −56.3 kJ/mol, respectively) but those of $NaAlH_4$ and $KAlH_4$ are quite different (−155 and −183.7 kJ/mol, respectively).

In contrast to the alkali metals, studies of the dehydrogenation of $Mg(AlH_4)_2$ by Fichtner et al.[12] showed that, at 163 °C, the dehydrogenation of the hydride proceeds according to eq 6 without the involvement of $[AlH_6]^{3-}$ as an intermediate phase. The resulting MgH_2 undergoes further dehydrogenation at 287 °C to produce magnesium metal that will react with aluminum at 400 °C to give Al_3Mg. The dehydrogenation of $Mg(AlH_4)_2$ is apparently exothermic, and thus, its direct rehydrogenation is precluded by thermodynamic constraints.

$$Mg(AlH_4)_2 \rightarrow MgH_2 + 2Al + 3H_2 \quad (6)$$

Rehydrogenation Reactions. The microreverse of the dehydrogenation of $NaAlH_4$ was first accomplished by Clasen,[39] who found that $NaAlH_4$ can be obtained in quantitative yields from tetrahydrofuran solutions of sodium hydride and activated aluminum powder at 150 °C and 13.6 MPa of hydrogen pressure in the presence of a catalytic amount of triethylaluminum. The solvent mediated, direct synthesis was improved to the point of commercial viability by Ashby et al.[40] Later, Dymova et al.[14] achieved the hydrogenation of the sodium system without solvent. Complete conversion to product was achieved at 270 °C under 17.5 MPa of hydrogen pressure in 2−3 h. The same group also reported the direct synthesis of $KAlH_4$ under analogous conditions. However, it was recently discovered that KH/Al can be hydrogenated to $KAlH_4$ under only 1.0 MPa of hydrogen in the 250−330 °C temperature range.[38] Apparently, the greater thermodynamic stability of $KAlH_4$, compared to $NaAlH_4$ discussed above, makes the enthalpy of hydrogenation significantly more exothermic and thus lowers the pressure required for hydrogenation.

Unlike sodium and potassium alanate, the enthalpy of hydrogenation of Li_3AlH_6 to $LiAlH_4$ is endothermic by 9 kJ/(mol of H_2). Since the entropy of hydrogenation must be negative, this is a nonspontaneous process under all conditions and thus direct hydrogenation cannot be achieved. However, the hydrogenation of LiH/Al to Li_3AlH_6 is weakly exothermic and could, in principle, be accomplished under very high pressure or at moderate pressures while also subjecting the material to some other means of overcoming the unfavorable entropic driving force. Recently, Wang et al.[41] reported evidence of the cyclic dehydrogenation and rehydrogenation between $LiAlH_4 \cdot 4THF$ and Li_3AlH_6, LiH, and Al. The dehydrogenation of half-cycles evolved about 4.0 wt % hydrogen below 130 °C. The decomposed products were rehydrogenated in tetrahydrofuran (THF). As Clasen[39] and Ashby et al.[40] found for the sodium system, the formation of a THF adduct circumvents the unfavorable thermodynamics associated with the formation of the pure alanate. However, the presence of the organic adduct introduces the additional problems of (1) a requisite side process to remove the adduct prior to dehydrogenation and (2) hydrogen contamination that must be overcome if the process is to be utilized as a practical method. The direct rehydrogenation of adduct-free $Mg(AlH_4)_2$ is also apparently precluded by thermodynamic constraints.

2.3.2. Doped $NaAlH_4$

Titanium compounds have long been known to catalyze the dehydrogenation of complex aluminum hydrides in solution. This effect was first reported by Wieberg et al. in 1951, who observed titanium catalyzed dehydrogenation of $LiAlH_4$ in a diethyl ether suspension.[42] Also, as discussed above, the commercial preparation of $NaAlH_4$ is accomplished through the catalyzed reaction of sodium hydride and activated aluminum powder in THF suspension.[40] The observation of a seemingly related catalytic effect of titanium for the dehydrogenation of $Mg_2Cl_3AlH_4$ in solution[43] prompted Bogdanović and Schwickardi to begin a systematic study of the catalytic effects of titanium in the reversible dehydrogenation of complex aluminum hydrides that was extended to the solid state. In 1995 they disclosed[44] that doping of $NaAlH_4$ with a few mole percent of titanium significantly enhanced the kinetics of the dehydrogenation and rehydrogenation processes. Remarkably, $NaAlH_4$ was found to undergo dehydrogenation in the *solid state* at 150 °C.[11] The conditions required for rehydrogenation were also dramatically reduced to 5 h at 170 °C and 15.2 MPa. Thus, this discovery provided a means of removing the "insurmountable" kinetic obstacle to harness the long recognized favorable thermodynamics of the reversible dehydrogenation of $NaAlH_4$ in the solid state. These findings suggested that sodium aluminum hydride could function as a rechargeable hydride under moderate conditions and might be developed for application as an on-board hydrogen storage material. However, the hydrogen capacities of their materials were found to quickly diminish upon cycling. Following the initial cycle, only 4.2 wt % of the 5.6 wt % that was eliminated could be restored under the moderate conditions employed in these studies. The hydrogen capacity was further diminished to 3.8 wt % after the second dehydriding cycle and reduced to only 3.1 wt % after 31 cycles.[11] Additionally, the dehydrogenation/rehydrogenation kinetics of these materials were inadequate for practical application as an on-board hydrogen storage material.

The original Bogdanović materials were prepared by evaporation of suspensions of $NaAlH_4$ in diethyl ether solutions of the soluble titanium compounds, titanium tetra-*n*-butoxide, $Ti(OBu^n)_4$, and β-titanium trichloride, β-$TiCl_3$. It was subsequently found that catalytic enhancement of $NaAlH_4$ also occurs upon mechanically mixing the titanium catalyst precursors with the aluminum hydride host.[45] The materials resulting from this method of preparation have kinetic and cycling properties that are much closer to those required for a practical hydrogen storage medium.[45,46] The kinetic improvement is illustrated in Figure 7, which compares the thermal programmed desorption (TPD) spectrum of undoped $NaAlH_4$ with that of hydride that was doped by both methods. It can be seen that the onset of rapid kinetics for the first dehydrogenation process occurs at ∼150 °C for hydride that is doped by the original method of Bogdanović and at a much lower, ∼120 °C, temperature for $NaAlH_4$ that is doped by mechanical milling. The discontinuity that occurs after elimination of ∼3.5 wt % hydrogen reflects the independence of the two dehydrogenation reactions. It is evident from Figure 7 that the two titanium-doped

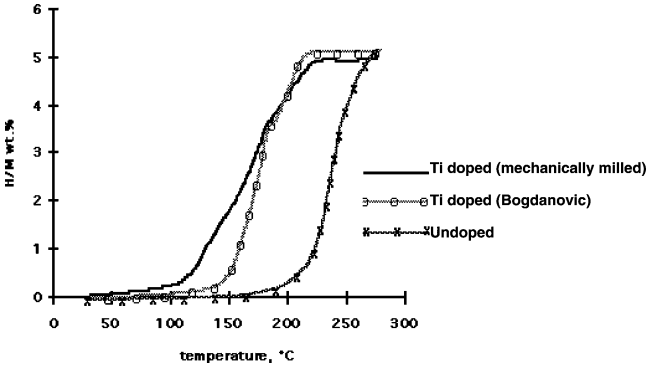

Figure 7. Thermal desorption (heating rate of 2 °C/min) from $NaAlH_4$.[267] Reprinted with permission from ref 267. Copyright 2001 Springer.

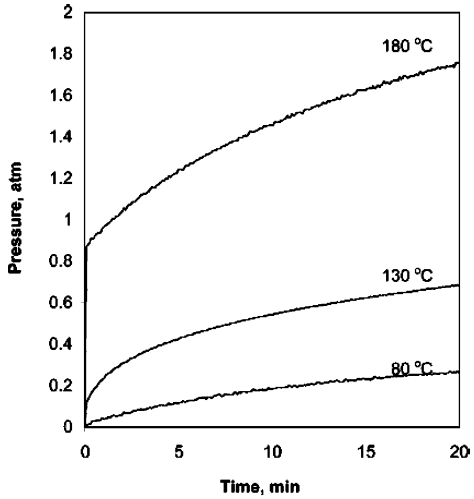

Figure 8. Progression of dehydrogenation upon heating from $NaAlH_4$ mechanically doped with 2 mol % $Ti(OBu^n)_4$ over the course of time at constant temperatures.[267] Reprinted with permission from ref 267. Copyright 2001 Springer.

materials differ primarily in their effectiveness in catalyzing the first dehydrogenation reaction. A more detailed kinetic study was carried out in which the release of hydrogen from samples of the homogenized material was monitored at constant temperatures.[47] As seen in Figure 8, the material undergoes rapid dehydrogenation at 130 °C and proceeds at an appreciable rate even at 80 °C.

Doping through mechanical milling of $NaAlH_4$ with dopant precursors is not only a more effective means of charging the hydride with catalyst but also activates the material through reduction of the average particle size.[45,48] It has, in fact, been demonstrated[49] that ball milling alone improves the dehydrogenating kinetics of undoped $NaAlH_4$. However, the introduction of catalysts enhances the kinetics far beyond those that are achieved by reducing the particle size.

A number of studies have compared the effectiveness of different titanium dopant precursors.[48,50−52] In addition to $TiCl_3$, $Ti(OBu^n)_4$, $TiCl_4$, and $TiBr_4$; TiF_3 has been proposed by several groups to be a highly effective, and perhaps a superior, dopant precursor.[53] Gross et al. have also shown that kinetic effects matching those achieved with the Ti(III) precursors are attained upon extended cycling of hydride doped with other titanium compounds that appear to be less effective dopant precursors during the initial cycles of dehydrogenation/rehydrogenation.[54] Recently, it was found

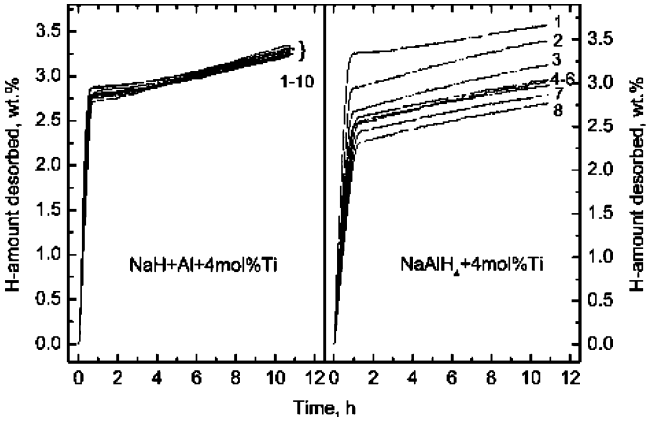

Figure 9. Comparison of the cycling dehydrogenation profiles between NaH + Al + 4 mol % Ti and $NaAlH_4$ + 4 mol % Ti. Both samples were prepared by mechanical milling under a H_2 atmosphere for 10 h.[55] Reprinted with permission from ref 55. Copyright 2004 American Chemical Society.

that even untreated, commercially available Ti powder can act as an effective dopant precursor upon prolonged mechanical milling.[55] However, in order to obtain a material with kinetics and stable hydrogen cycling capacities that match those of hydride doped with Ti(III) or Ti(IV) precursors, it is necessary to mill the Ti powder with mixtures of NaH/Al rather than $NaAlH_4$. Figure 9 compares the cycling dehydrogenation performance of materials that were both prepared through milling with Ti powder under a H_2 atmosphere for 10 h. No signs of degradation in either hydrogen capacity of dehydrogenation kinetics were seen for the material prepared from NaH/Al. Unfortunately, the potential for an improved hydrogen capacity upon elimination of the doping byproducts resulting from the Ti(III) precursors was not realized, as only 3.3 wt % hydrogen was obtained from dehydrogenation at 150 °C. The low hydrogen cycling capacity is, at least partly, due to the very slow kinetics of the second dehydrogenation step, which are inferior to those of materials prepared from the Ti(III) or Ti(IV) precursors.

Outstanding kinetic enhancement of hydrogen cycling kinetics as well as hydrogen cycling capacities have been observed for $NaAlH_4$ doped with Ti·0.5THF nanoparticles.[56,57] However, the practical application of the nanoclusters is precluded by the difficulty and cost of their preparation. Additionally, the kinetic enhancement of the materials doped with the nanoparticles has been found to steadily diminish upon hydrogen cycling.[57]

Comparative studies of other metal halides as dopant precursors for treating $NaAlH_4$ have shown that similar levels of kinetic enhancement of the reversible dehydrogenation can be achieved upon doping with chlorides of zirconium, vanadium, and several lanthanides.[46,48] Lower levels of catalytic activity have been reported to occur in hydride that was charged with $FeCl_2$ and $NiCl_2$,[48] as well as with carbon.[49] It was recently reported that ball milling the hydride with 2 mol % $ScCl_3$, $CeCl_3$, or $PrCl_3$ gives rise to a material with rehydrogenation kinetics and storage capacities that are significantly greater than those of the Ti-doped hydride.[58] In addition, the rehydrogenation of the scandium-doped system was found to require lower pressures than the titanium-doped material. Although these dopants were found to reduce rehydrogenation times by a factor of ∼2 at 10.0 MPa and a factor of ∼10 at 5.0 MPa, the high kinetic performance upon cycling at the lower pressure was found to persist only with the cerium-doped material. Wang et al.[59] studied Sc-doped $NaAlH_4$ at higher dopant loadings and

Table 3. Hydrogen Storage Properties of Alanates

reaction	hydrogen wt % (ideal)	obs hydrogen wt % first dehyd	obs hydrogen wt % rehyd	conditions: temp (°C) (pressure (MPa)) first dehyd	conditions: temp (°C) (pressure (MPa)) rehyd	exp ΔH_{dehyd} (kJ/(mole of H_2))	ref
$LiAlH_4 = LiH + Al + {}^3/_2H_2$	8.0	8.0		201		5.8	26
$LiAlH_4 = {}^1/_3Li_3AlH_6 + {}^2/_3Al + H_2$	5.3	5.3		187−218		−9.1	26, 34
$LiAlH_4 = {}^1/_3Li_3AlH_6 + {}^2/_3Al + H_2$ (with Ti dopant)	5.3	5.3		25			255
$Li_3AlH_6 = 3LiH + Al + {}^3/_2H_2$	5.6	5.6		228−282		27.0	26, 34
$Li_3AlH_6 = 3LiH + Al + {}^3/_2H_2$ (with Ti dopant)	5.6	5.5		100−120			256
$NaAlH_4 = NaH + Al + {}^3/_2H_2$	5.6	5.6	5.6	265	27.0 (17.5)	56.5	14, 27, 32, 36, 37
$NaAlH_4 = NaH + Al + {}^3/_2H_2$ (with Ti dopant)	5.6	5.0	3.5−4.3	160	12.0−15.0 (11.5)	56.5	43, 48, 67, 257
$NaAlH_4 = {}^1/_3\alpha\text{-}Na_3AlH_6 + {}^2/_3Al + H_2$	3.7	3.7		210−220		36.0	27, 32
$NaAlH_4 = {}^1/_3\alpha\text{-}Na_3AlH_6 + {}^2/_3Al + H_2$ (with Ti dopant)	3.7	3.7	3.5	90−150	12.0 (11.5)	37.0, 40.9	48, 67, 257
$\beta\text{-}Na_3AlH_6 = 3NaH + Al + {}^3/_2H_2$	3.0	3.0		250		46.8	27, 32, 36, 37
$\beta\text{-}Na_3AlH_6 = 3NaH + Al + {}^3/_2H_2$ (with Ti dopant)	3.0	3.0	2.9	100−150	12.0 (11.5)	47.0	43, 46, 48
$Na_2LiAlH_6 = 2NaH + LiH + Al + {}^3/_2H_2$	3.5	3.2	2.8−3.2	170−250		53.0	60, 61
$Na_2LiAlH_6 = 2NaH + LiH + Al + {}^3/_2H_2$ (with Ti dopant)	3.5	3.0	2.6−3.0	170−250		53.0	60, 61
$KAlH_4 = KH + Al + {}^3/_2H_2$	4.3	3.5	2.6−3.7	290	25.0−33.0 (0.10)	∼86.0	38
$Mg(AlH_4)_2 = MgH_2 + 2Al + 3H_2$	6.9	6.9		163−285			12
$Mg(AlH_4)_2 = MgH_2 + 2Al + 3H_2$ (with Ti dopant)	6.9	6.9		140−200			12

observed fast hydrogenation kinetics and minimal hydrogen capacity losses over cycling.

It has been found that titanium and zirconium catalysts are quite compatible and can exert their differing catalytic roles in concert to optimize the dehydrogenation/rehydrogenation behavior of $NaAlH_4$.[48] Bogdanović et al.[48] also found that catalytic activity can be optimized through charging the hydride with dual dopants. They discovered a synergistic effect in hydride that is doped with a combination of $Ti(OBu^n)_4$ and $Fe(OEt)_2$. The resulting materials exhibit dehydrogenation and rehydrogenation kinetics that are superior to those observed for the hydride that is charged with either of the dopants alone.

2.3.3. Other Doped Alanates

Bogdanović and Schwickardi found that the kinetic enhancement upon Ti-doping can be extended to the reversible dehydrogenation of $LiNa_2AlH_6$ to LiH, 2 NaH, and Al.[11] They found the mixed alkali metal alanate to have significantly lower plateau pressure at 211 °C and thus a higher ΔH_{dehy} than Na_3AlH_6. Fossdal et al.[60] conducted PCT measurements over the 170−250 °C temperature range and, from the van't Hoff plot of their data, determined ΔH_{dehy} to be 56 kJ/mol. Graetz et al.[61] observed that the undoped mixed alanate will also undergo reversible dehydrogenation. They found that while doping 4 mol % $TiCl_3$ results in a highly pronounced kinetic enhancement, it has no effect on the thermodynamic properties of the hydride.

Titanium has also been found to enhance the dehydrogenation kinetics of $LiAlH_4$.[62] Balema et al.[62] found that $LiAlH_4$ could be transformed into Li_3AlH_6 and Al at room temperature upon the addition of 3 mol % $TiCl_4$ upon 5 min of mechanical milling. The dehydrogenation of Li_3AlH_6 to LiH and Al was found by Chen et al.[63] to occur at temperatures as low as 100 °C upon doping the hydride with 2 mol % $TiCl_3$. Blanchard et al.[64] reported that addition of a few mole percent VCl_3 can also reduce the thermal decomposition temperature of $LiAlH_4$ by 60 °C.

Chen et al. also reported XRD evidence[63] for partial rehydrogenation of the resulting mixture of LiH/Al to an uncharacterized "intermediate phase". However, attempts to reproduce this result were unsuccessful. Recently, Ritter et al.[41] confirmed the findings of the earlier studies of Ti-doped lithium alanate. These investigators also reported that the kinetics of the formation of the THF adduct of $LiAlH_4$ from the ball milling of THF solutions of dehydrogenated material were improved by the addition of 0.5 mol % of a titanium catalyst.

Fichtner et al.[12] studied the kinetic effects of $Mg(AlH_4)_2$ doped with 2 mol % $TiCl_3$ and mechanically milled for up to 100 min. The studies showed that the peak decomposition temperature was reduced in the presence of the titanium dopant. The starting point of the first decomposition step shifted to lower temperatures; however, complete dehydrogenation to MgH_2 still requires heating to ∼200 °C.

2.4. Prospectus

Although there are instances of transition-metal-doped alanates that have hydrogen cycling capacities, thermodynamic properties, or kinetic performances that are suitable for onboard vehicular hydrogen storage (Table 3), no material meets all three criteria. Sodium alanate, however, has a combination that most closely approaches those that are requisite of the long sought, "holy grail" material. Overall, a number of thermodynamic, kinetic, capacity, and safety issues cloud the future practical application of this class of materials.

2.4.1. Thermodynamic Considerations

The dehydrogenations of both $LiAlH_4$ and $Mg(AlH_4)_2$ are irreversible. Thus, thermodynamic constraints would allow only $NaAlH_4$ to be utilized as an onboard hydrogen storage material that could be recharged by direct hydrogenation. However, $LiAlH_4$ and $Mg(AlH_4)_2$ might find application in a system in which they were utilized as "chemical hydrides" involving their regeneration through an off-board chemical process.

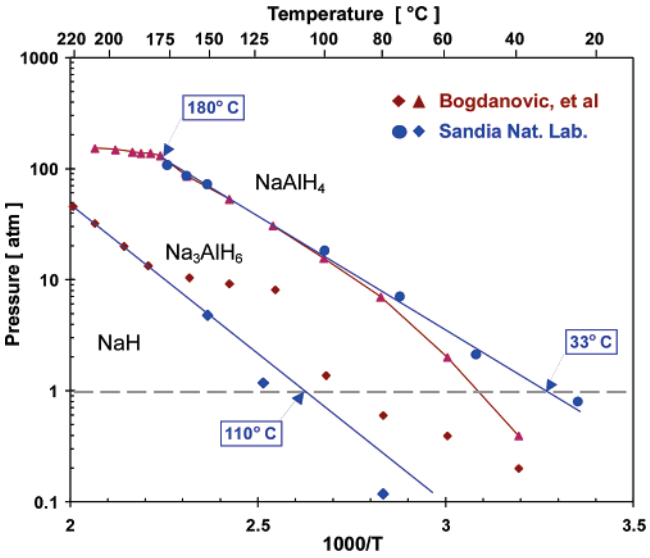

Figure 10. Van't Hoff plot of equilibrium pressures as a function of temperature for the $NaAlH_4 \leftrightarrow {}^1/_3(\alpha\text{-}Na_3AlH_6) + {}^2/_3Al + H_2$ and the $\alpha\text{-}Na_3AlH_6 \leftrightarrow 3NaH + Al + {}^3/_2H_2$ reactions. Samples were doped with 2 mol % each of $Ti(OBu^n)_4$ and $Zr(OPr^i)_4$.[267] Reprinted with permission from ref 267. Copyright 2001 Springer.

A van't Hoff plot of the data obtained from PCT studies of Ti-doped $NaAlH_4$ is presented in Figure 10. From this data,[52] the enthalpy of the dehydrogenation of $NaAlH_4$(s) to Na_3AlH_6 and Al has been determined to be 37 kJ/(mol of H_2). This value is in line with the predictions of the studies discussed earlier. In accordance with this value, the temperature required for an equilibrium hydrogen pressure of 0.1 MPa has been determined[65] as 33 °C and highly practical hydrogen plateau pressures of 0.2 and 0.7 MPa have been found at 60 and 80 °C, respectively.[52] Unfortunately, the equilibrium hydrogen plateau pressures of the Na_3AlH_6/NaH + Al + H_2 equilibrium in the 70−100 °C temperature range are insufficient for utilization in a PEM fuel cell system in which the heat of the steam exhaust would be used to drive hydrogen release for the storage material. As seen in Figure 10, a temperature of 110 °C is required to attain a plateau pressure of 0.1 MPa. Thus, unless a system has an additional means of heating the storage material, the potential hydrogen storage capacity of sodium alanate is limited to 3.6 wt %. As discussed in the previous section, Na_2LiAlH_6 and $KAlH_4$ have even lower plateau pressures than Na_3AlH_6 and thus offer no storage potential in this type of system.

2.4.2. Kinetic Considerations

Ti-doped $LiAlH_4$, $NaAlH_4$, and $Mg(AlH_4)_2$ all undergo dehydrogenation at appreciable rates at temperatures at or below 100 °C, suggesting their possible application as hydrogen carries for onboard PEM fuel cells. The recent finding of further kinetic enhancement of $NaAlH_4$ through Sc-doping demonstrates that even faster rates of dehydrogenation can be achieved. However, it should be noted that scandium is expensive and may not be the best option for practical on board hydrogen storage.

The kinetics of rehydrogenation for Ti-doped $NaAlH_4$, the only candidate material for onboard recharging, are a much more daunting challenge to any effort for its practical development. As advances have been made in improving the kinetics of rehydrogenation, the problem of managing the heat generated from this highly exothermic process has come to light.[66] Clearly, a very high performance heat exchanger will be required to adequately remove the large amounts of heat that would be discharged during the short (~5 min) time that is considered to be acceptable for practical onboard refueling.

2.4.3. Hydrogen Cycling Capacity Performance

The long-term cycling of mixtures of NaH/Al that were doped with 2 wt % TiF_3 has been studied through 100 cycles (hydrogenation 150 °C, 11.4 MPa; dehydrogenation 160 °C).[67] A release of 3.4 wt % of hydrogen was obtained in the first dehydrogenation half-cycle. Upon cycling, the storage capacity showed a steady increase to the 4.0 wt % limit that was achieved by the fourth dehydrogenation half-cycle. This capacity remained through 40 cycles before the onset of a steady decrease resulting in a loss of capacity from 4.0 to 3.5 wt % by the end of the 100th cycle. Synchrotron powder X-ray diffraction and Rietveld profile fitting analysis of Ti-doped (NaH + Al) after 100 cycles showed the presence of additional phases, which are apparently linked to the observed diminishing dehydrogenation characteristics. Decreases in dehydrogenation kinetics and the total amount of released hydrogen over a number of cycles parallel the appearance of the intermediate phase, Na_3AlH_6, in the prolonged cycling samples. This indicates a reduction in the effectiveness of the Ti-dopant for the hydrogenation of Na_3AlH_6 to $NaAlH_4$. Clearly, development of methods for stabilizing the hydrogen storage capacity upon long-term cycling would be necessary before this material could be used for practical applications. Moreover, the 3.5−4.0 wt % cycling capacity falls far short of the current U.S. Department of Energy capacity target that is thought to be necessary for a practically viable, onboard hydrogen storage material.

2.4.4. Safety

The main safety concern associated with the alanates is their high reactivity with water. The heat of the hydrolysis reactions can drive the thermal decomposition of the hydrides. However, the pressure rise associated with introduction of small amounts of contaminant water into the system during recharging would not constitute a significant fraction of the pressure rating of any credible container. However, contact of this hydride system with a larger amount of water upon accidental tank rupture in a wet environment is clearly a safety concern. This hazard must be eliminated either through system engineering or chemical modification of the hydride.

2.4.5. General Outlook

In view of the thermal management issue associated with onboard recharging of Ti-doped sodium alanate and the irreversibility of the dehydrogenation of $LiAlH_4$ and $Mg(AlH_4)_2$, it appears that a practical hydrogen storage system based on alanates would most likely require off-board recharging. Currently, only sodium alanate can be directly charged under hydrogen pressure and, thus, until new, highly economical chemical processes for the regeneration of alanates are developed, it is the only member of this class of materials which is a plausible candidate for practical hydrogen storage for vehicular applications. Despite the problems discussed above, Ti-doped sodium alanate to date stands as *the* hydrogen storage material with the best combination of materials properties that are suited for vehicular hydrogen storage. However, its cycling hydrogen capacity is only 3−4 wt %. Thus, barring the discovery of

the "holy grail" hydrogen storage material, the practical application of these materials will await a time when there is public acceptance of vehicles that are lighter weight and/or capable of cruise ranges that are significantly shorter than 300 miles.

3. Amides

3.1. Synthesis

The pioneering efforts of Chen et al.[68] in 2002 motivated extensive studies on the reversible hydrogen storage properties of lithium amide.[69−91] Alkali-metal amides have traditionally been used as reagents in synthetic organic chemistry. The original experiments for the synthesis of the wide variety of amides and their basic reactions related to hydrogen were systematically summarized by Bergstrom and Fernelius.[92] Some amides, such as sodium amide ($NaNH_2$) and potassium amide (KNH_2), were prepared as early as the beginning of the 1800s by Gay-Lussac and Thénard.[93] Lithium amide ($LiNH_2$) was synthesized in 1894 by Titherley.[94] A compound with the formula "Li_3NH_4" was reported to be obtained in 1910 by Dafert and Miklauz upon the heating (at 220−250 °C) of lithium nitride, Li_3N, under hydrogen.[95] The next year, this compound was identified by Ruff and Georges to be a mixture, or possibly a solid solution, of lithium amide and lithium hydride, i.e., $LiNH_2 + LiH$.[96] On heating this mixture to 340−480 °C, the amide is converted into imide and ammonia, and the latter immediately combines with the hydride, forming lithium imide and hydrogen. Hence, the total reaction is given by eq 7:[92]

$$LiNH_2 + LiH \leftrightarrow Li_2NH + H_2 \quad (7)$$

The investigators supported their hypothesis by the known decomposition of lithium amide into lithium imide at 240−450 °C and by the fact that at a slightly higher temperature lithium hydride reacts with ammonia to form lithium amide.

Other amides have also been reported:[92] $Mg(NH_2)_2$ was synthesized by the reactions of Mg_3N_2 or Mg with ammonia (gas and liquid). However, the time required for reaction completion was on the order of years. The solid−gas reaction of MgH_2 with ammonia was recently employed to prepare the single phases $Mg(NH_2)_2$ and MgNH.[97,98] Also, the following amides have been reported: $RbNH_2$, $CsNH_2$, Ca−N−H,[68,99,100] Li−Ca−N−H,[101] Li−Al−N−H,[102−105] Na−Mg−N−H,[106] Na−Ca−N−H,[107] Mg−Ca−N−H,[108−110] Li−Mg−Ca−N−H,[111] and hydrides of variable nitrides.[112] Li−Mg−N−H[72,74,97,98,101,113,114] is described in detail in the following section. A quaternary hydride having the approximate composition $Li_3BN_2H_8$ ($LiBH_4$ together with 2 mol of $LiNH_2$) has been synthesized by mechanical milling and/or by heating the mixed powders.[102,115−118] Furthermore, the combination of $LiBH_4$ and $LiNH_2$ by mechanical milling also forms the other new series of quaternary hydrides Li_2BNH_6 (together with 1 mole of $LiNH_2$) and $Li_4BN_3H_{10}$ (together with 3 mol of $LiNH_2$), depending on the combination ratios. In addition, $(LiNH_2)_x(LiBH_4)_{1-x}$ was synthesized for the compositions $x = 0.33-0.80$.[119−120]

3.2. Structure

3.2.1. $LiNH_2$

The crystal structure of $LiNH_2$, shown in Figure 11, was first determined by X-ray diffraction in 1951[121] and subsequently by neutron diffraction in 1972.[122] These structures are peculiar because the distance between the nearest nitrogen and hydrogen atoms, d_{N-H}, is only 0.70 Å, which is much shorter than $d_{N-H} = 1.022$ Å for monomeric/unsolvated $LiNH_2$, recently reported.[123] The crystal structure of $LiNH_2$ was reinvestigated using powder neutron diffraction with high sensitivity. The compound was seen to crystallize in the tetragonal space group $I\bar{4}$ with lattice constants of $a = 5.03442(24)$ Å and $c = 10.25558(52)$ Å. Hydrogen atoms occupy the 8g site. The two values of d_{N-H} are 0.986 and 0.942 Å, respectively, and the H−N−H bond angle (∠H−N−H) is about 99.97°.[124] A deuterated sample, $LiND_2$, was also found to crystallize in the same space group with lattice constants of $a = 5.03164(8)$ Å and $c = 10.2560(2)$ Å. The two determined values of dN−D are similar (0.967(5) and 0.978(6) Å), and the ∠D−N−D is 104.0(7)°. These structural parameters are close to those of the isoelectronic water molecule.[125]

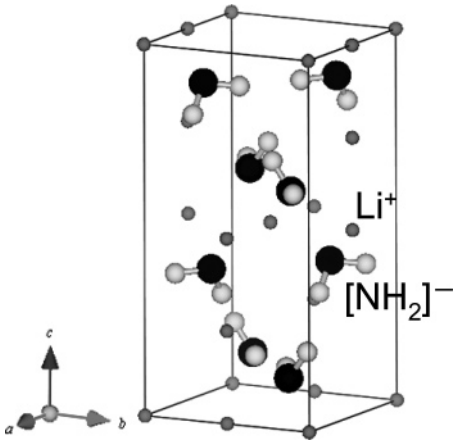

Figure 11. Crystal structure of $LiNH_2$.[121,122] Large (black), medium (white), and small (gray) spheres indicate nitrogen, hydrogen, and lithium, respectively.

First-principles calculations for $LiNH_2$ were performed using the ultrasoft pseudopotential method based on density functional theory.[113,126,127] As indicated in Figure 12, the partial density of states for $LiNH_2$ shows little contribution of the Li orbitals to the occupied states and, therefore, it is likely that the Li atom is ionized as Li^+ ion. The occupied states consist of N-2s, N-2p, and H-1s orbitals that are strongly localized around the complex anion $[NH_2]^-$. The lowest-energy state is composed of the N-2s and H-1s orbitals. In the middle-energy region, the N-2p orbital hybridizes with the H-1s orbital. In the higher occupied states, the N-2p orbital is dominant and has a nonbonding character.[113,126,127] The electronic structure based on the refined structure of the $LiNH_2$ was also calculated. The total density of states (DOS) shows a band gap of 3.48 eV between the valence and conduction bands, which indicates a nonmetallic nature. The band gap is larger than that of 3.2 eV shown by Miwa et al.[126] Charge density analysis shows a strong degree of ionicity, and the average valence state of Li is about 0.86^+.[124] It was also reported that the N atom bonds unequally with the two H atoms in $LiNH_2$. As a result, $LiNH_2$ can dissociate in two almost equivalent transient steps: (1) $Li^+ + [NH_2]^-$ and (2) $[LiNH]^- + H^+$. The reaction of the relevant species may evolve NH_3 as a transient gas in the ($LiNH_2 + LiH$) system.[128]

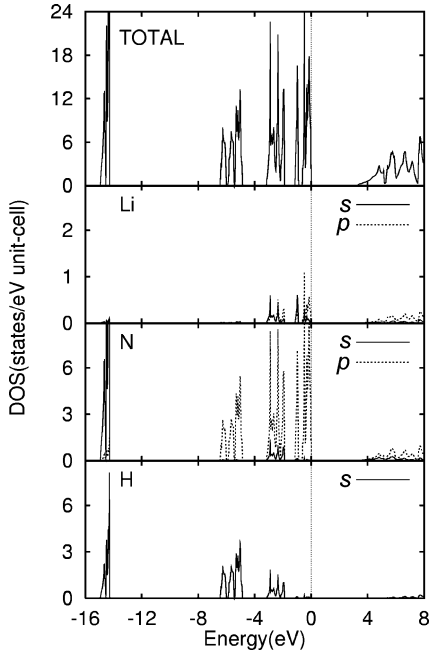

Figure 12. Total and partial densities of states for $LiNH_2$.[113,126] The origin of the energy is set to be the top of the valence states. Reprinted with permission from ref 113. Copyright 2004 Springer.

3.2.2. Li_2NH

The crystal structure of Li_2NH has also been reinvestigated. Synchrotron X-ray diffraction data indicates that Li_2NH has the cubic (anti-fluorite-type) space group $Fm\bar{3}m$ with a lattice constant of $a = 5.0742(2)$ Å at 22 °C. Hydrogen atoms randomly occupy the 48h site around the N atoms, and the value of d_{N-H} is 0.80(16) Å. The charge density distribution around $[NH]^{2-}$ in Li_2NH is almost spherical.[129] From the neutron diffraction data, two models have been proposed: model "I" with $Fm\bar{3}m$, 48h-site occupation for hydrogen, and d_{N-H} of 0.79(2) Å; model "II" with $F\bar{4}3m$, 16e-site occupation for hydrogen, and $d_{N-H} = 0.82(6)$ Å. Both models have a lattice constant of $a = 5.0769(1)$ Å.[130] Combined analyses of X-ray and neutron diffractions found that an order−disorder transition occurs in $Li_2NH(D)$ near 87 °C. Below that temperature, Li_2ND can be described to the same level of accuracy as a disordered cubic space group $Fd\bar{3}m$ with a lattice constant of $a = 10.09-10.13$ Å. Refinement of the data collected at −173 °C gives a d_{N-D} of 0.977 Å. Both the N and H atoms fully occupy the 32e sites. The H atoms are tetrahedrally coordinated to vacant 8b sites, and the N atoms are tetrahedrally coordinated to Li atoms on the 8a and 48f sites. The high-temperature structure has the cubic (anti-fluorite-type) space group $Fm\bar{3}m$ with a lattice constant of $a = 5.0919$ Å at 127 °C. Deuterium atoms randomly occupy the 192l sites with a d_{N-H} of 0.904 Å.[131]

The electronic structure of Li_2NH at room temperature was studied using synchrotron X-ray diffraction and the maximum entropy method (MEM).[129] The number of electrons within the sphere around the Li^+ and $[NH]^{2-}$ is estimated from the obtained charge density distribution. As a result, the ionic charge is expressed as $[Li^{0.99+}]_2[NH]^{1.21-}$. Therefore, it is confirmed that Li_2NH is also an ionic compound.[129] The ground-state (low-energy) electronic structures, closely related to quantum effects, of hydrides with $[NH]^{2-}$ are important matters for investigation, and experimental and theoretical studies have been carried out.[132−135]

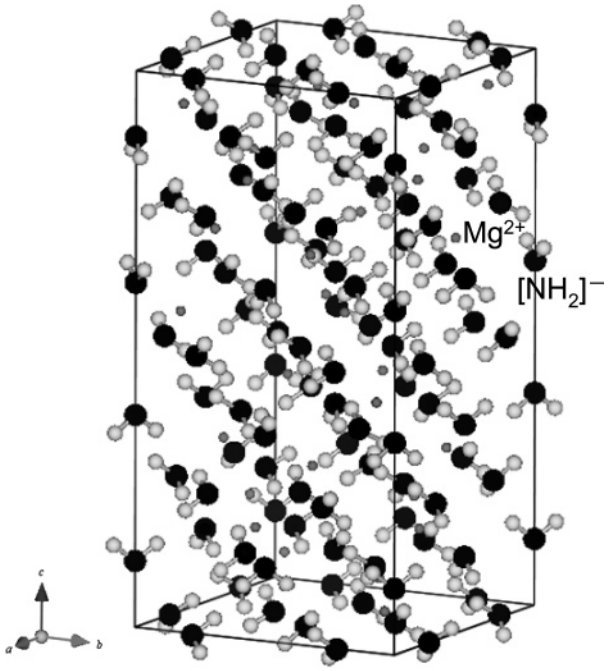

Figure 13. Crystal structure of $Mg(NH_2)_2$.[268] Large (black), medium (white), and small (gray) spheres indicate nitrogen, hydrogen, and magnesium, respectively.

3.2.3. $Mg(NH_2)_2$

The structure for $Mg(ND_2)_2$ determined by neutron diffraction is seen in Figure 13. The data refinement proceeded smoothly in the tetragonal space group $I41/acd$ with lattice constants of $a = 10.3758(6)$ and $c = 20.062(1)$ Å. However, powder synchrotron X-ray diffraction data indicates that the symmetry may be lower. The values of d_{N-H} are in the range of 0.95(1)−1.07(1) Å, and ∠H−N−H is about 101(1)−107(2)°.[125]

3.2.4. $Li_4BN_3H_{10}$

Mechanical milling of $LiNH_2$ and $LiBH_4$ in varying combination ratios results in the formation of a series of new quaternary hydrides: Li_2BNH_6, $Li_3BN_2H_8$, and $Li_4BN_3H_{10}$. The crystal structure of $Li_4BN_3H_{10}$ is cubic (BCC) space group $I213$ with lattice constants of $a = 10.673(2)$ Å,[117] $a = 10.66445(1)$ Å,[118] and $a = 10.679(1)-10.672(1)$ Å.[136] It should be emphasized that $Li_4BN_3H_{10}$ is an ionic crystal which is composed of Li^+ and both $[NH_2]^-$ and $[BH_4]^-$ complex anions in the molar ratio 1:3. The crystal structure is shown in Figure 14. $[NH_2]^-$ has a nearly tetrahedral bond angle (∠H−N−H = 106°), while $[BH_4]^-$ has an almost ideal tetrahedral geometry (∠H−B−H = 108−114°). Three symmetry-independent Li atom sites are surrounded by $[NH_2]^-$ and $[BH_4]^-$ in various distorted tetrahedral configurations, one by two N atoms and two B atoms, another by four N atoms, and the third by three N atoms and one B atoms. The Li configuration around N resembles a distorted saddlelike configuration, while that around B is nearly tetrahedral, similar to those in $LiBH_4$ and $LiNH_2$, respectively (8a + 24c-sites for H, N−H = 0.83−0.86 Å, B−H = 1.08−1.11 Å).[136] The other quaternary hydrides, Li_2BNH_6 and $Li_3BN_2H_8$, are also predicted to have similar structures composed of Li^+ and mixtures of $[NH_2]^-$ and $[BH_4]^-$.[117]

The calculation of the total and partial density of states for $Li_4BN_3H_{10}$ indicates that an approximately 4 eV gap separates the valence and conduction bands with primarily ionic bonding among Li^+, $[NH_2]^-$, and $[BH_4]^-$ species.[137]

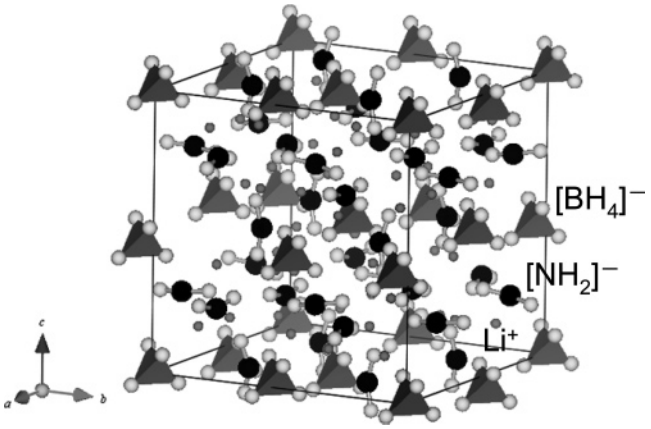

Figure 14. Crystal structure of $Li_4BN_3H_{10}$.[117] Large (black), medium (white), and small (gray) spheres indicate nitrogen, hydrogen, and lithium, respectively. Boron is centered in $[BH_4]^-$ tetrahedra.

3.3. Dehydrogenation and Rehydrogenation Reactions

The sequential dehydrogenation and rehydrogenation reactions of $LiNH_2$ proceed according to eq 8.[68,92] The first and second reactions release 5.5 and 5.2 wt % hydrogen, respectively. It was proposed[72,74] that partial substitution of

$$LiNH_2 + 2LiH \leftrightarrow Li_2NH + LiH + H_2 \leftrightarrow Li_3N + 2H_2 \quad (8)$$

Li with more electronegative elements would weaken the bonding between Li^+ and $[NH_2]^-$. Lithium amide with partial Mg substitution was synthesized from the Li−Mg alloys, and the dehydrogenation reactions were investigated.[113] The dehydrogenation reaction from $LiNH_2$ (+LiH) without the partial Mg substitution begins at approximately 277 °C upon heating at the rate of 10 °C/min under argon. However, the temperature is drastically lowered to around 100 °C with increasing Mg concentrations.[113] Thus, cation substitution is an effective method for decreasing the dehydrogenation temperatures of $LiNH_2$ (and also of $LiBH_4$).[138]

A theoretical approach to reducing the dehydrogenation temperature of $LiNH_2$ by partial element substitution was investigated. Results of the (Li, Mg)NH_2 study showed that the bonding nature of Li−N and N−H is the same as that in $LiNH_2$, but the bond strength of N−H was reduced. The difference can be used to explain the experimental observation that the dehydrogenation temperature was reduced by Mg substitution.[139] The relative strength of the metal−N ionic bonding has been found to be a key factor to explain the effects of the substitutes.[140]

The optimization of composites of amide and hydride, for example, the composite of $Mg(NH_2)_2$ and LiH,[141−151] is also important for enhancing the dehydrogenation reaction. The dehydrogenation mechanism (ammonia mediated mechanism) was proposed by Hu and Ruckenstein[152] and Ichikawa et al.[76] First, amide ($LiNH_2$ in eq 8) decomposes into imide (or even into nitride) continuously with increasing temperature, at which only ammonia can be desorbed. Second, ammonia reacts with the coexisting hydride (LiH in eq 8), resulting in dehydrogenation. Chen et al.[69] and Lu et al.[153] have reported another dehydrogenation mechanism (redox or acid−base mechanism). In this mechanism, the hydrogen in $LiNH_2$ is positively charged ($H^{\delta+}$), but it is negatively charged ($H^{\delta-}$) in LiH. The pair of $H^{\delta+}$ and $H^{\delta-}$ combines to easily form molecular hydrogen (H_2), and simultaneously, $N^{\delta-}$ and $Li^{\delta+}$ combine to form Li_3N. The mechanism of the dehydrogenation reaction is still under discussion.

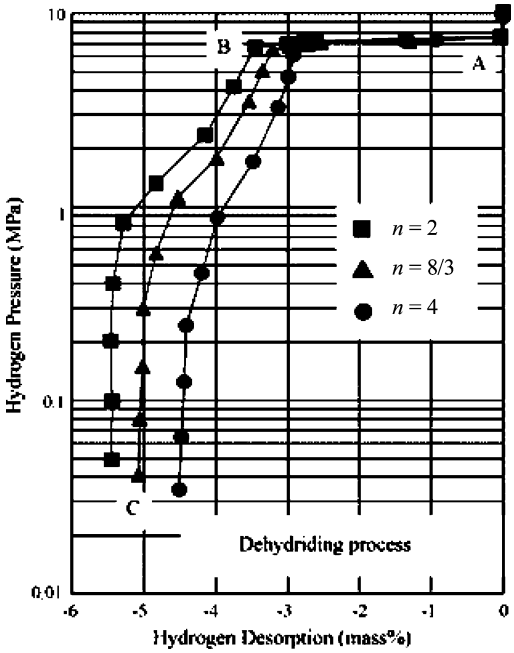

Figure 15. Hydrogen pressure−composition ($p-c$) isotherms of the composite of $Mg(NH_2)_2 + n$LiH ($n = 2$, $^8/_3$, and 4) during the dehydrogenation reaction at 250 °C. Points A, B, and C mark the beginning of the plateau region, the end of the plateau region, and the end of the sloping region on the isotherms, respectively.[157] Reprinted with permission from ref 157. Copyright 2007 Elsevier.

Considering the ammonia-mediated process mentioned above, the composite of $Mg(NH_2)_2$ and LiH has been selected as one of the appropriate combinations for decreasing the dehydrogenation temperature.[97,98] The complex $Mg(NH_2)_2$ decomposes at a lower temperature compared to that of $LiNH_2$, and also LiH reacts rapidly with ammonia from $Mg(NH_2)_2$. For example, the following overall reaction (eq 9) has been proposed:[97,154]

$$Mg(NH_2)_2 + 4LiH \leftrightarrow {}^1/_3Mg_3N_2 + {}^4/_3Li_3N + 4H_2 \quad (9)$$

According to eq 9, the calculated hydrogen capacity of the system is 9.1 wt %. In the heating process, the main weight loss in the composite of $Mg(NH_2)_2$ and 4LiH was observed below 230 °C, which is lower than that of the composite of $LiNH_2$ and 2LiH. The weight loss in the composite of $Mg(NH_2)_2$ and 4LiH at 527 °C was at approximately 7 wt %, which is 77% of the calculated value. The dehydrogenation reaction of eq 9 was precisely investigated by hydrogen pressure−composition ($p-c$) isotherm (PCT) and X-ray diffraction measurements.[155]

The dehydrogenation reactions of composites of $Mg(NH_2)_2$ and LiH were reported for other composition ratios of LiH. These reactions proceed as seen in eqs 10 and 11:[98,114,141]

$$Mg(NH_2)_2 + {}^8/_3LiH \leftrightarrow {}^1/_3Mg_3N_2 + {}^4/_3Li_2NH + {}^8/_3H_2 \quad (10)$$

$$Mg(NH_2)_2 + 2LiH \leftrightarrow Li_2Mg(NH)_2 + 2H_2 \quad (11)$$

According to eqs 10 and 11, a total of 6.9 and 5.6 wt % hydrogen are predicted to be released.

The dehydrogenation and rehydrogenation reactions of the composite shown in eqs 9−11 were systematically investi-

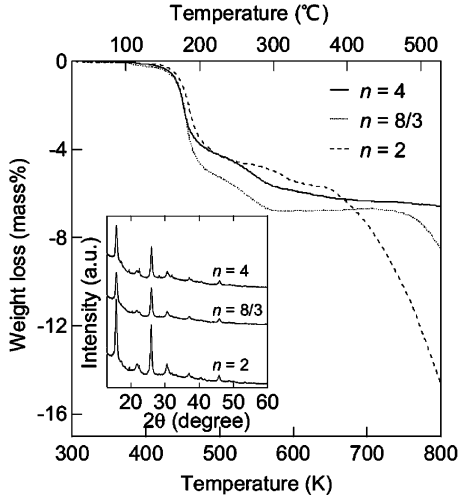

Figure 16. Thermal desorption (thermogravimetry) from the composites of $Mg(NH_2)_2 + nLiH$ ($n = 2$, $^8/_3$, and 4) under helium flow at 0.1 MPa. The inset shows the powder X-ray diffraction profiles (Cu Kα) of the samples heated to 240 °C (after the main dehydrogenation reaction around 187 °C).[156] Reprinted with permission from ref 156. Copyright 2005 Japan Institute of Metals.

gated by thermogravimetry, PCT, and X-ray diffraction measurements.[156,157] The features of the $p-c$ isotherms at 250 °C were found to be similar. In addition, the amounts of hydrogen desorbed increase with decreasing composition ratios of LiH in the composites: 4.5, 5.1, and 5.4 wt % of hydrogen for eqs 9−11, respectively (Figure 15). However, the mass spectroscopy profiles around 187 °C clearly indicate an increase in production of gas-phase ammonia with decreasing composition ratios of LiH. The composition ratios obviously affect the suppression of the ammonia release at temperatures higher than 330 °C (Figure 16).[156,157] Therefore, the practical composition ratios of the composites of $Mg(NH_2)_2$ and LiH can be suitably *tuned* on the basis of the actual application conditions (Figure 17).

3.4. Prospectus

The hydrogen storage properties of amides and their related materials are summarized in Table 4. Additional information is also available.[158] Studies[159,160] of the cyclic dehydrogenation and rehydrogenation of composites of $Mg(NH_2)_2$ and LiH through 270 cycles of the reaction in eq 11 revealed a 25% reduction of the hydrogen storage capacity. Ammonia formation accounts for only 7% of the capacity loss. The cause of additional capacity loss is unclear at present. For the composites of $Mg(NH_2)_2$ and LiH, the temperature needed to form appreciable amounts of ammonia was reported to be much higher than that required for hydrogen release. The ammonia concentration in the desorbed hydro-

Table 4. Hydrogen Storage Properties of Amides and Their Related Materials

reaction	hydrogen wt % ideal	hydrogen wt % obs (first dehyd)	hydrogen wt % *o*bs (rehyd)	conditions: temp (°C) (pressure (MPa)) first dehyd	conditions: temp (°C) (pressure (MPa)) rehyd	theor/exp ΔH_{dehyd} (kJ/(mole of H_2))	ref
$LiNH_2 + 2LiH = Li_3N + 2H_2$	10	9	5−5.5	170−400	195−285 (0.01 −1.0)	T 80.5−99	68−70, 73, 77, 79, 80, 82, 83, 86−89, 126−128, 134
$Li_2NH + LiH = Li_3N + H_2$	5.5	∼5.5		350−400		T 148−165	
$LiNH_2 + LiH = Li_2NH + H_2$	6.5(−6.85)	5.5	3−6.8	170−300	195−285 (0.01 −1.0)	T 40.9−74.8 E 60−65.6	
$CaNH + CaH_2 = Ca_2NH + H_2$	2.1	3.5	1.9		500−550 (0.001−0.1)	E 88.7	68, 99, 100, 107, 112
$Ca(NH_2)_2 + CaH_2 = 2CaNH + 2H_2$	3.5					T 57	
$2CaNH + CaH_2 = Ca_3N_2 + 2H_2$	2.7	2.4	∼1.1		500−600 (<0.68)	T 115	
$Ca(NH_2)_2 + 2LiH = CaNH + Li_2NH + 2H_2$	4.5	4.5	2.5	120−300	180 (3.0)		
$2Ca(NH_2)_2 + 2NaH = 2NaNH_2 + Ca-Na-H + H_2$		1.1	1	120−270	∼200 (7.0)	E 55	
$Mg(NH_2)_2 + 2MgH_2 = Mg_3N_2 + 4H_2$	7.4	∼7		RT−450		T 2−3.5	97, 108, 112, 145
$Mg(NH_2)_2 + MgH_2 = 2MgNH + 2H_2$	4.9	4.8		65−310		T 43	
$Mg(NH_2)_2 + nLiH = Li_2Mg(NH)_2 + (n-2)LiH + 2H_2$							98, 114, 141, 146, 148, 150, 151, 154, 156, 157
$n = 2$	5.6		5.4	140−280	250 (0.1−8.0)	E 38.9−44.1	
$n = {}^8/_3$	5.2		5.1				
$n = 4$	4.6		4.5				
$Mg(NH_2)_2 + {}^8/_3LiH = {}^1/_3Mg_3N_2 + {}^4/_3Li_2NH + {}^8/_3H_2$	6.9	∼7		140−280			
$Mg(NH_2)_2 + 4LiH = {}^1/_3Mg_3N_2 + {}^4/_3Li_3N + 4H_2$	9.1	∼7		140−520			
$Mg(NH_2)_2 + 1.5NaH$		2.2	2.2	RT−160	160−200 (0.3 psi to 3 psi)	E 80	106, 108, 110, 111
$2Mg(NH_2)_2 + 4CaH_2 = CaMg_2N_2 + Ca_2NH + CaNH + 7H_2$	5	4.9	∼1	60−510	200−250 (10.0)		
$Mg(NH_2)_2 + CaH_2 = MgCa(NH)_2 + 2H_2$	4.1	0.5−3.9		80−400			
$Mg(NH_2)_2 + Ca(NH_2)_2 + 4LiH = Li_4MgCa(NH)_4 + 4H_2$	5	2.7−3.0	2.7	220 (0.1−50)			
$2LiNH_2 + LiAlH_4 = Li_3AlN_2 + 4H_2$	9.6	4.1		RT−600			102−105
$2LiNH_2 + 2LiAlH_4 = 2Li_2AlNH + 5H_2$		∼8		50−350			
$LiNH_2 + 2LiAlH_4 = 2Al + Li_2NH + LiH + 4H_2$	8.2	8.1		85−320			
$6LiNH_2 + 2Li_3AlH_6 = 6Li_2NH + 2Al + 9H_2$	7.4	7.1	7.1	150−300	300 (13.6)		
$8LiNH_2 + 4Li_3AlH_6 = 4Li_2NH + 6LiH + 2Li_3AlN_2 + 2Al + 15H_2$	7.6	6.9	3−4	100−500	200−300 (0.004−10.0)	T 23 E 29	
$2LiNH_2 + LiBH_4 = Li_3BN_2 + 4H_2$	11.9	>10	1.4	250−380	RT−150 (8.4)	T 23	102, 115, 116, 118−120

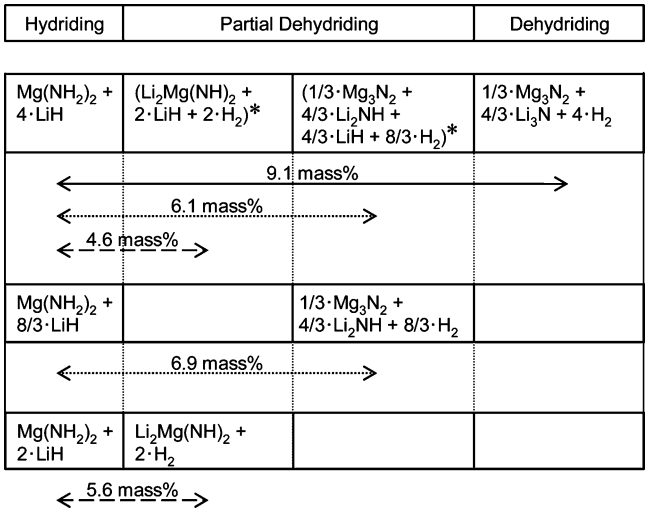

Figure 17. Summary of the dehydrogenation and rehydrogenation reactions of the composite of $Mg(NH_2)_2 + n$LiH ($n = 2$, $^8/_3$, and 4). *Some intermediate phases are now being investigated.[156] Reprinted with permission from ref 156. Copyright 2005 Japan Institute of Metals.

gen increased with the temperature from 180 ppm at 180 °C to 720 ppm at 240 °C.[159,160]

It was recently reported that the dehydrogenation reaction closely relates to the diffusion of Li^+ into the cation sites of $Mg(NH_2)_2$.[161] The reaction process in the $Mg(NH_2)_2-LiH$ system is showed schematically in Figure 18. Li^+ diffuses from LiH to $Mg(NH_2)_2$ crystal and then decomposes $[NH_2]^-$ into $[NH]^{2-}$ and H^+. The created H^+ in $Mg(NH_2)_2$ is attracted to LiH and combined with H^-, resulting in formation of H_2 gas. The hydrogenation probably proceeds by the reverse of this process. Furthermore, it seems plausible that the low temperature, reversible dehydrogenation and rehydrogenation of the $Mg(NH_2)_2-LiH$ system is facilitated by the similarity of the imide and amide structures.

Suitable tuning of composition ratios and creating novel micro-/nanostructures are needed to reduce the amount of ammonia, increase the cyclic durability, and promote the Li^+ diffusion.

4. Borohydrides (Tetrahydroborate)

4.1. Synthesis

The first report of a pure alkali metal borohydride (tetrahydroborate) appeared in 1940 by Schlesinger and Brown,[162] who synthesized lithium borohydride ($LiBH_4$) by the reaction of ethyl lithium with diborane (B_2H_6). The direct reaction (eq 12) of the corresponding metal hydride with

$$2MH + B_2H_6 \rightarrow 2MBH_4, \quad \text{where M} = \text{Li, Na, K, } {}^1/_2\text{Mg, etc.} \quad (12)$$

diborane in etheral solvents under suitable conditions produces high yields of the borohydrides.[163]

Direct synthesis from the metal, boron, and hydrogen (eq 13) at 550−700 °C and 3−15 MPa H_2 has been reported to

$$M + B + 2H_2 \rightarrow MBH_4, \quad \text{where M} = \text{Li, Na, K, } {}^1/_2\text{Mg, etc.} \quad (13)$$

yield the lithium salt, and this method is generally applicable to group IA and IIA metals.[164]

Transition, lanthanide, and actinide metal borohydride complexes have been prepared by substitution of $[BH_4]^-$ for a halide ion. The use of an excess of the alkali borohydride is often necessary to achieve complete substitution. In a number of cases, substitution of a halide ligand by a borohydride has been accompanied by a corresponding reduction in the oxidation state of the metal ion. For example,[165,166] the reaction of $MgCl_2$ with an alkali metal borohydride results in the metathesis reaction seen in eq 14.

$$MgCl_2 + 2MBH_4 \rightarrow Mg(BH_4)_2 + 2MCl, \quad \text{where M} = \text{Li or Na} \quad (14)$$

The solid-state metathesis reaction of various borohydrides has been demonstrated[167] by mechanical milling of metal halides with an alkali borohydride in an inert gas atmosphere based on the above reactions. For example, zinc borohydride, $Zn(BH_4)_2$, has been synthesized[168] by the reaction of $ZnCl_2$ and $NaBH_4$.

The direct synthesis of borohydride complexes[169] has been accomplished by the reaction of an alkali or alkaline earth hydride with a triethylamine borane complex under argon atmosphere. The mixture is heated while stirring, and the triethylamine adduct of the borohydride is formed. This direct method was applied for the synthesis of $Mg(BH_4)_2$.[170]

4.2. Structure

The structure of borohydrides is a subject of controversy, as different structures have been determined from X-ray and neutron diffraction studies. Detailed descriptions of the crystal and electronic structures of the B−H systems are available.[74,171−198]

4.2.1. $LiBH_4$

The phases of $LiBH_4$ were determined by means of synchrotron X-ray diffraction at low and high temperature. An endothermic (4.18 kJ/mol) structural transition from the orthorhombic to the hexagonal structure is observed at 118 °C. The hexagonal structure melts at 287 °C with a latent heat of 7.56 kJ/mol. This structure is still under discussion, since the theoretical calculation of the phonon density of states has shown unusual features.[180,181] Both phase transitions are reversible, although a small temperature hysteresis is observed.

The crystal structure of $LiBH_4$ was originally determined by Harris and Meibohm.[177] They found that the unit cell contains four molecules and has the dimensions $a = 7.1730$ Å, $b = 4.4340$ Å, and $c = 6.7976$ Å at 258 °C and calculated a density of 0.669 g/cm^3. Each Li^+ ion was seen to be surrounded by four $[BH_4]^-$ ions in a tetrahedral configuration. The $[BH_4]^-$ is strongly deformed: two hydrogen atoms are at a bond length of $d_{B-H} = 1.30$ Å, one is at 1.28 Å, and one is at 1.44 Å (4c+8d-sites for H).[199] The crystal structure of $LiBH_4$ has been recently redetermined by synchrotron X-ray diffraction at room temperature and at 135 °C, as shown in Figure 19. At room temperature the hydride

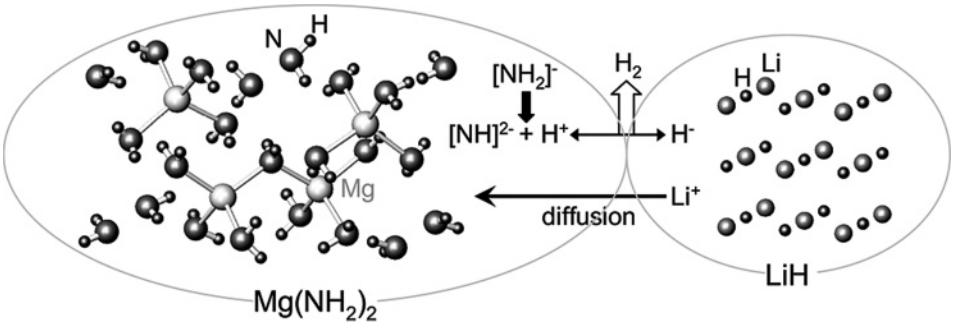

Figure 18. Schematic view of the reaction process in the composite of $Mg(NH_2)_2 + LiH$.[161]

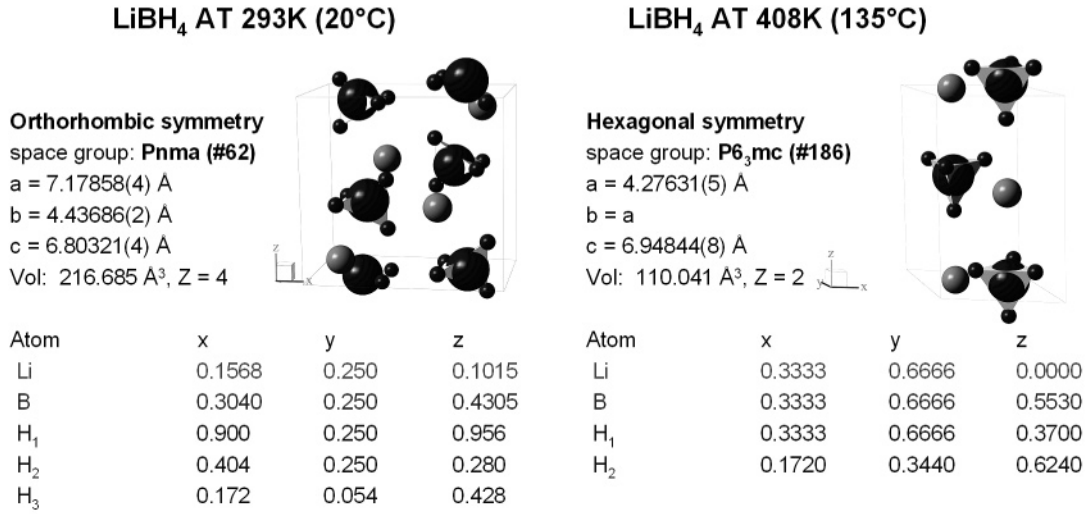

Figure 19. Low- and high-temperature structures of $LiBH_4$ determined from X-ray diffraction. Large, medium, and small spheres indicate boron, lithium, and hydrogen, respectively.[178,179,203] Reprinted with permission from ref 203. Copyright 2007 Elsevier.

crystallizes in the orthorhombic space group *Pnma* (a = 7.17858(4) Å, b = 4.43686(2) Å, c = 6.80321(4) Å).[178,179] The complex $[BH_4]^-$ anions were found to be aligned along two orthogonal directions and are strongly distorted with respect to bond lengths (d_{B-H} = 1.04(2)−1.28(1) Å) and bond angles ($\angle$H−B−H = 85.1(9)−120.1(9)°). As the temperature is increased, the structure undergoes a phase transition and becomes hexagonal (space group *P*6*mc*, a = 4.27631(5) Å, c = 6.94844(8) Å at T = 135 °C).[178,179] The $[BH_4]^-$ tetrahedra align along c, become more symmetric (d_{B-H} = 1.27(2)−1.29(2) Å, $\angle$H−B−H = 106.4(2)−112.4(9)°) and show displacement amplitudes that are consistent with dynamic disorder about their trigonal axis.

4.2.2. $NaBH_4$

Davis and Kennard[184] performed neutron powder diffraction studies at room temperature on $NaBD_4$. The Na^+ cation and $[BH_4]^-$ anion were found to crystallize with a NaCl-type structure. Although only the lattice parameters had been obtained in an earlier X-ray diffraction study,[185] these early investigators mentioned that the sodium and boron atoms may form a body-centered tetragonal array and that the hydrogen atoms could lie on a primitive tetragonal lattice. The structure of $NaBD_4$ was recently found to belong to space group $P\bar{4}21c$.[186]

4.2.3. Other Borohydrides

Neutron diffraction[187] of KBD_4 shows a tetrahedral array of hydrogen atoms about the boron atom with d_{B-H} of 1.219 Å, and the crystal is face-centered cubic at room temperature.[188] $Mg(BH_4)_2$ is predicted to crystallize in the orthorhombic space group *Pmc*21 with a fascinating two-dimensional arrangement of Mg^{2+} and $[BH_4]^-$.[200] The Rietveld analysis of the diffraction pattern of $Ca(BH_4)_2$ can be interpreted as space group *Fddd*, and the calculated pattern closely reproduces the measured one. The intensity of the unassigned peaks is very weak; thus, the studied sample is thought to be almost a single phase of $Ca(BH_4)_2$. The B−H bond lengths and the H−B−H bond angles are d_{B-H} = 1.11−1.13 Å and $\angle$H−B−H = 102−119°, respectively. Each Ca^{2+} is surrounded by six octahedrally coordinated $[BH_4]^-$, and each $[BH_4]^-$ has three Ca^{2+} neighbors.

4.3. Dehydrogenation and Rehydrogenation Reactions

Overall dehydrogenation of alkali metal borohydrides proceeds as follows:

$$M(BH_4) \rightarrow MH + B + {}^3/_2H_2 \qquad (15\text{-}1)$$

$$\text{or} \qquad A(BH_4) \rightarrow AB + 2H_2 \qquad (15\text{-}2)$$

Alkaline earth borohydrides dehydrogenate according to eqs 16-1 to 16-3.

$$M(BH_4)_2 \rightarrow MH_2 + 2B + 3H_2 \qquad (16\text{-}1)$$

$$\text{or} \qquad M(BH_4)_2 \rightarrow MB_2 + 4H_2 \qquad (16\text{-}2)$$

$$\text{or} \qquad M(BH_4)_2 \rightarrow {}^{2}/_{3}MH_2 + {}^{1}/_{3}MB_6 + {}^{10}/_{3}H_2 \qquad (16\text{-}3)$$

$LiBH_4$ liberates three of the four hydrogen atoms from the compound upon melting at 280 °C and decomposes into LiH and boron.[201] The thermal desorption spectrum exhibits four endothermic peaks. The peaks are attributed to a polymorphic transformation around 110 °C, melting at 280 °C, the hydrogen desorption (50% of the hydrogen was desorbed ("$LiBH_2$") around 490 °C), and the desorption of three of the four hydrogen atoms at 680 °C. Only the third peak (hydrogen desorption) is pressure dependent. The calculated enthalpy ($\Delta H = -177.4$ kJ/(mol of H_2)) and entropy ($\Delta S = 238.7$ J/(K·mol of H_2)) of decomposition are not in agreement with the values deduced from indirect measurements of the stability.[202] The value of the entropy is too high and cannot be explained because the standard entropy for hydrogen is 130 J/(K·mol of H_2). Additives to the borohydride (such as SiO_2)[179] lower the hydrogen desorption temperature for $LiBH_4$ by approximately 100 K. Although $LiBH_4$ is well-known to react with glass at elevated temperatures, recent studies of the isotherms have suggested that the effect of SiO_2 is a catalytic effect and not a destabilization of the complex.[203]

As shown in Figure 20, the dehydrogenation process of $LiBH_4$ at a low heat ramping rate (0.5 °C/min) exhibits three distinct desorption peaks.[199] This is an indication that the desorption mechanism involves several intermediate steps. This was recently explained by the formation of a borohydride cluster as an intermediate phase,[204] and Raman spectroscopy and XRD have delivered some evidence[205] for the existence of $Li_2B_{12}H_{12}$ as an intermediate phase of the hydrogen desorption reaction of $LiBH_4$.

Figure 21 summarizes the energy levels for the hydrogen desorption reaction of $LiBH_4$ considering the enthalpy of the reactants. The most stable state is $LiBH_4$ in the low-temperature structure *Pnma*, which is transformed into the high-temperature modification ($P6_3mc$) at 118 °C, followed by melting around 280 °C. Subsequently, desorption of hydrogen is observed, via the intermediate phase(s) discussed in the previous paragraph, resulting in LiH and solid boron. Due to the high stability of LiH ($\Delta H_{LiH} = -181.4$ kJ/(mol of H_2)), its dehydrogenation proceeds at temperatures above 727 °C and is, therefore, usually not accessible in technical applications.

Alkali metal borohydrides are usually prepared by chemical methods, e.g., by the reaction of the metal hydride with diborane in a solvent ($2LiH + B_2H_6 \rightarrow LiBH_4$ in THF). The dehydrogenation reaction from $LiBH_4$ is reversible, and the end products lithium hydride (LiH) and boron absorb hydrogen at "600 °C under 35 MPa" or at "690 °C under 20 MPa" to form $LiBH_4$.[138,203] The result is in agreement with the claim in Goerrig's patent[164] about the direct formation of $LiBH_4$ from the elements. The mechanism of the absorption of hydrogen by LiH and B to form $LiBH_4$ is under investigation, and the two following reaction paths have been proposed:

(1) LiH and B react with each other, forming an intermediate state, which is "filled up" with hydrogen, finally resulting in $LiBH_4$.

(2) Boron and hydrogen react to form diborane, which is known to spontaneously react with alkali hydrides, delivering alkali metal borohydrides[206] (e.g., in the case of $NaBH_4$).

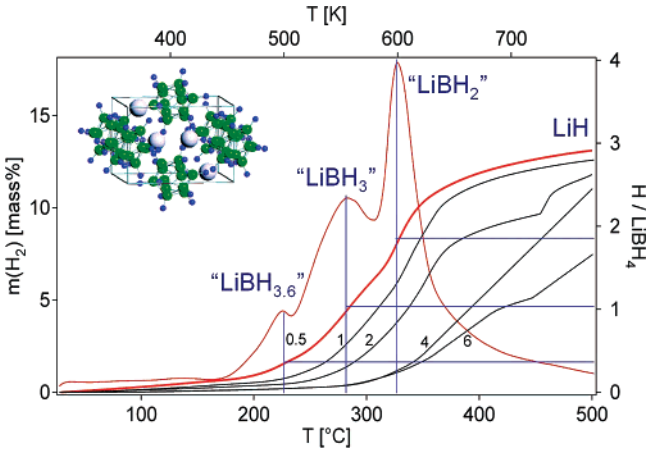

Figure 20. Integrated thermal desorption (heating rate of 0.5−6 °C/min) from $LiBH_4$ measured at various heating rates shown in the figure. The differential curve for the lowest heating rate of 0.5 °C/min is given together with the hypothetical compositions at the peak maxima.[203] The structure of an intermediate phase[204,205] is shown as the inset. Reprinted with permission from ref 203. Copyright 2007 Elsevier. Inset reprinted with permission from ref 204. Copyright 2006 American Physical Society.

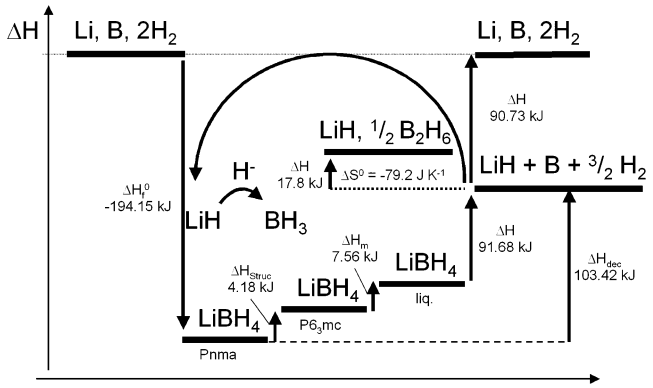

Figure 21. Schematic enthalpy diagram of the phases and intermediate products of $LiBH_4$.[203] Reprinted with permission from ref 203. Copyright 2007 Elsevier.

The counterargument for the latter reaction path is that the reaction of hydrogen with boron is endothermic ($\Delta H° = 35.6$ kJ/(mol of H_2), $\Delta S° = -79.2$ J/(K·mol of H_2))[207] and will, therefore, only proceed at high temperatures and pressures (driven by entropy). The diborane in the gas-phase reacts upon cooling of the sample with the solid LiH and the LiH transfers an H^- to the BH_3 to exothermically form $LiBH_4$ following eqs 17 and 18.

$$3H_2 + 2B \rightarrow (BH_3)_2$$
at high temperature and high pressure (17)

$$2Li^+H^- + (BH_3)_2 \rightarrow 2Li^+[BH_4]^-$$
upon cooling of the reactor (18)

The release of diborane during dehydrogenation of borohydrides is observed[203] probably as a concurrent reaction to the liberation of hydrogen. To form diborane during desorption, an H^- atom is transferred from the borohydride complex to the positively charged Li, leaving LiH and a neutral BH_3 molecule, which is the basic element of diborane (shown in eq 16). Diborane evolution during desorption is thus likely to occur, but this does not provide evidence for its formation from the elements. Apart from the unfavorable thermody-

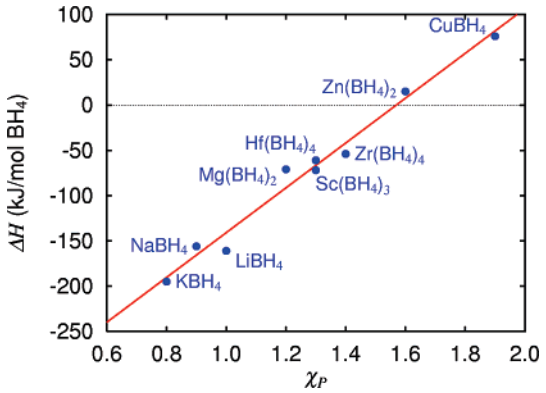

Figure 22. Correlation between the heats of formation of metal borohydrides $M(BH_4)_n$, ΔH_{boro}, and the Pauling electronegativities of M, χ_P. The estimation of ΔH_{boro} is based on the following reaction: $(1/n)M + B + 2H_2 \rightarrow (1/n)M(BH_4)_n$. Zero-point energy contributions to ΔH_{boro} are approximately taken into consideration.[211] Reprinted with permission from ref 211 (http://link.aps.org/abstract/PRB/v74/p45126). Copyright 2006 by the American Physical Society.

namics to form diborane, a kinetic barrier contributes to the general inert behavior of boron. It is not clear whether this behavior originates from the particular modification of boron (passivation by oxides, etc.) or from intrinsic properties of the material. Support for the first point is given by the fact that the formation of $LiBH_4$ occurs if one starts from LiH and nanodispersed B obtained from dehydrogenation of borohydride.[138]

In the concurrent desorption reaction (second reaction), neutral H is removed from the complex, leaving charged $[BH_3]^-$, and 2H are recombined to H_2. However, $[BH_3]^-$ is highly unstable according to recent calculations.[208] Therefore, Ohba et al.[204] calculated the stability of complexes consisting of several boron and hydrogen atoms. It was found that the influence of the charge is weakened by its "distribution" over several atoms and the complex is stabilized.

A mechanism of the total rehydrogenation process could not be given until now, and the discussion above makes clear the importance of this knowledge. If formation of $LiBH_4$ is initiated by the formation of diborane, catalysts promoting this reaction have to be found. On the other hand, the second reaction is catalyzed by additives promoting the interaction between LiH and B. Recently, it was discovered that the kinetic barrier for the formation of borohydrides is drastically reduced if metal−boron compounds (e.g., MgB_2) are used instead of pure boron as starting materials.[209] An investigation of the interaction among these borates, hydrogen, and lithium hydride might provide us with further information to unravel the rehydrogenation mechanism of borohydrides. The scientific understanding of the mechanism of the thermal hydrogen desorption from $LiBH_4$ and the hydrogen absorption reaction remains a challenge and requires additional studies.

4.4. Electronegativity–Stability Correlation

It was reported that[210] there is a correlation between the electronegativity of the cation and the frequency of the bending and stretching modes of hydrogen in the anion, as well as the melting temperature of the complex. The thermodynamic stabilities for the series of metal borohydrides $M(BH_4)_n$ (M = Li, Na, K, Mg, Sc, Cu, Zn, Zr, and Hf; n = 1−4) have been systematically investigated by first-principles calculations.[211,212] The results indicated that the bond between M^{n+} and $[BH_4]^-$ in $M(BH_4)_n$ is ionic, and the charge transfer from M^{n+} to $[BH_4]^-$ is responsible for the stability of $M(BH_4)_n$. As shown in Figure 22, the heat of formation of the $M(BH_4)_n$ depends linearly on the Pauling electronegativity χ_p of M:

$$\Delta H_{boro} = 248.7\chi_p - 390.8 \quad \text{in the units of kJ/(mol of } BH_4) \quad (19)$$

The thermal desorption analyses[167,211] indicate that $LiBH_4$, $NaBH_4$, and KBH_4 desorb hydrogen to the elemental hydride of the cation. Multistep hydrogen desorption reactions are observed for $Mg(BH_4)_2$, $Sc(BH_4)_3$, and $Zr(BH_4)_4$. On the other hand, $Zn(BH_4)_2$ desorbs hydrogen and borane to elemental zinc due to the instabilities of zinc hydride and boride.

Quite interestingly, the thermal desorption temperatures, T_d, of $M(BH_4)_n$ decrease with increasing χ_p. T_d is not related to the enthalpy formation of $M(BH_4)_n$ (ΔH_{boro}) but rather to the enthalpy decomposition (enthalpy difference between the elementary metal hydride and the complex hydride).[213] The values can be estimated by using ΔH_{boro} (eq 19) and reported data for decomposed products, which correlates with observed T_d. The same correlation between observed T_d and the averaged electronegativity of the metal cation MM′ exists in the double cation $MM'(BH_4)_n$ system.[214] Therefore, the electronegativity of the metal cation might be a good indicator for estimations of the T_d of $M(BH_4)_n$.

4.5. Prospectus

The alkali metal and alkaline-earth metal borohydrides belong to a class of materials with gravimetric hydrogen densities that are among the highest known today (Tables 1 and 5). Although these complex hydrides have been known to exist for more than 50 years, only limited data on their

Table 5. Hydrogen Storage Properties of Borohydrides

reaction	hydrogen wt % ideal	hydrogen wt % obs (first dehyd)	hydrogen wt % *o*bs (rehyd)	conditions: temp (°C) (pressure (MPa)) first dehyd	conditions: temp (°C) (pressure (MPa)) rehyd	theor/exp ΔH_{dehyd} (kJ/(mole of H_2))	ref
$LiBH_4 = LiH + B + {}^3/_2H_2$	13.9	13.5	5−10	180−500	600−650 (7.0 −35.0)	T 52−76	138, 179, 181, 199, 211, 212, 258, 259, 260, 261, 262
$LiBH_4 = {}^1/_{12}Li_2B_{12}H_{12} + {}^5/_6LiH + {}^{13}/_{12}H_2$	10	~11		430−460		T 56	204, 205, 263
$LiBH_4 + {}^1/_2MgH_2 = LiH + {}^1/_2MgB_2 + 2H_2$	11.4	6−10	8−10	300−585	315−450 (0.5 −2.0)	T 46/E 40.5	260, 261, 264, 265
$LiBH_4 + 2LiNH_2 = Li_3BN_2 + 4H_2$	11.9	>10	1.4	250−380	RT−150 (8.4)	T 23	102, 115, 116, 118, 119, 120, 262
$Ca(BH_4)_2 = {}^2/_3CaH_2 + {}^1/_3CaB_6 + {}^{10}/_3H_2$	9.6					T 32	266
$M(BH_4)_n$: M = variable alkali, alkaline-earth, and transition metals	see each ref						167, 200, 211, 214, 253

dehydrogenation and rehydrogenation properties is available due to their high reactivity and, therefore, the difficulty of handling such materials. Fedneva et al.[215] reported results of the thermal hydrogen desorption from $LiBH_4$ in 1964. Stasinevich et al.[201] investigated the thermal hydrogen desorption under various hydrogen pressures in order to estimate the thermodynamic hydrogen sorption properties.

The heat of hydride formation will, apart from the hydrogen storage capacity, determine the practicality of a compound to be used as a hydrogen storage material. Furthermore, the heat of formation of complex hydrides is not necessarily large; for example, $Al(BH_4)_3$ delivers the hydrogen spontaneously below room temperature. Few studies have focused on the complex hydride $Al(BH_4)_3$.[216] It has a high gravimetric hydrogen density of 17 wt % and the highest known volumetric hydrogen density of 150 $kg \cdot m^{-3}$. Also, it has a melting point of −65 °C and is liquid at room temperature. Besides covalent hydrocarbons, ammonia, and water, this is the only liquid hydride at room temperature. New complexes, such as $Ca(BH_4)_2 \cdot Al(BH_4)_3$, may provide opportunity for new systems with even larger hydrogen densities and the desired stabilities for the application.

The dehydrogenation reaction of MBH_4 (M = Li, Na, and K) in the microwave heating process has been investigated recently, in which only $LiBH_4$ was heated up and an almost theoretical amount of hydrogen was desorbed above 380 K.[217,218] A novel microwave heating process might be useful for complex hydrides having low thermal conductivity, because microwave energy can be absorbed directly by the materials.

5. Conclusion

The present review provides an overview of the progress of the complex hydrides for hydrogen storage. Some other recent reviews and original articles are also informative.[219−253]

Over the past decade, tremendous progress has been made toward the development of complex hydrides for potential use as an onboard hydrogen carrier. This approach to hydrogen storage, which was once thought to be "impossible", has been brought to the threshold of commercial viability. Alanates are attractive because of the rapid kinetics of their dehydrogenation and rehydrogenation. Borohydrides have extremely high available hydrogen mass percents that meet the current, highly stringent U.S. Department of Energy targets. Amides have reaction kinetics and hydrogen mass percents which both approach practical viability. However, all of the complex hydrides currently have practical limitations that must be overcome. Alanates have insufficient reversible capacity; borohydrides suffer from unacceptably slow kinetics and also from undesirable evolution of diborane; and amides are plagued by both capacity and kinetic limitations as well as undesirable evolution of ammonia. Additionally, the problem of thermal management on recharging is common to all complex hydrides. In view of the great progress that has been made, it can be anticipated that further advances will be made toward the development of group I and group II complex hydrides. Recently, the frontier of research in this area has been extended to the combinations of transition metal salts of these compounds. This new area of research may lead to the identification of materials which are free from the above-mentioned problems.

6. Acknowledgments

We gratefully acknowledge financial support received from the Office of Hydrogen Fuel Cells and Infrastructure Technology of the U.S. Department of Energy; the Japanese Ministry of Economy, Trade and Industry (METI); the Japanese Ministry of Education, Culture, Sports, Science and Technology (MEXT); the New Energy and Industrial Technology Development Organization (NEDO), Japan; the Swiss Federal Office of Energy (BFE); and EU FP6 IP NESSHY. Valuable collaboration and communication with the groups of Drs. S. Towata and K. Miwa in Toyota Central R&D Labs; Drs. H.-W. Li, T. Sato, and K. Ikeda and Mr. K. Kikuchi and Ms. N. Warifune in IMR; Dr. R. Zidan of Savannah River National Lab; Drs. B. Hauback and H. Brinks of the Institute for Energy Technology, Norway; and Dr. G. Sandrock are highly appreciated.

7. Note Added after ASAP Publication

This paper was published ASAP on September 12, 2007. A production error in Table 4 was corrected, and the paper was reposted on September 14, 2007.

8. References

(1) Sandrock, G.; Suda, S.; Schlapbach, L. *Hydrogen in Intermetallic Compounds II, Topics in Applied Physics*; Springer-Verlag: 1992; Vol. 67 (5), p 197.
(2) Sandrock, G.; Yurum, Y. *Hydrogen Energy Systems: Production and Utilization of Hydrogen and Future Aspects*; NATO ASI Series; Kluwer Academic Publishers: 1994; p 253.
(3) Carpetis, C.; Peshka, W. *Int. J. Hydrogen Energy* **1980**, *5*, 539.
(4) Agarwal, R. K.; Noh, J. S.; Schwarz, J.; Davini, R. *Carbon* **1987**, *25*, 219.
(5) Dillion, A. C.; Jones, K. M.; Bekkedahl, T. A.; Kiang, C. H.; Bethune, D. S.; Heben, M. *Nature* **1997**, *386*, 377.
(6) Park, C.; Anderson, P. E.; Chambers, A.; Tan, C. D.; Hidago, R.; Rodriquez, N. M. *J. Phys. Chem. B* **1999**, *103*, 10572.
(7) Liu, C.; Fan, Y. Y.; Liu, M.; Wei, Y. L.; Lu, M. Q.; Cheng, H. M. *Science* **1999**, *286*, 1127.
(8) Suda, S.; Sandrock, G. *Z. Phys. Chem.* **1994**, *183*, 149.
(9) Ye, Y.; Ahn, C. C.; Witham, C.; Fultz, B.; Liu, J.; Rinzler, A. G.; Colbert, D.; Smith, K. A.; Smalley, R. E. *Appl. Phys. Lett.* **1999**, *74*, 2307.
(10) Pinkerton, F. E.; Wicke, B. G.; Olk, C. H.; Tibbetts, G. G.; Meisner, G. P.; Meyer, M. S.; Herbst, J. F. *J. Phys. Chem. B* **2000**, *104* (40), 9460.
(11) Bogdanović, B.; Schwickardi, M. *J. Alloys Compd*. **1997**, *1*−*9*, 253.
(12) Fichtner, M.; Fuhr, O.; Kircher, O. *J. Alloys Compd*. **2003**, *356*−*357*, 418.
(13) Huot, J.; Boily, S.; Guther, V.; Schulz, R. *J. Alloys Compd.* **1999**, *283*, 304.
(14) Dymova, T. N.; Eliseeva, N. G.; Bakum, S. I.; Dergachev, Y. M. *Dokl. Akad. Nauk SSSR*. **1974**, *215*, 1369.
(15) Lauher, J. W.; Dougherty, D.; Herley, P. J. *Acta Crystallogr*. **1979**, *B35*, 1454.
(16) Sklar, N.; Post, B. *Inorg. Chem*. **1967**, *6*, 699.
(17) Bel'skii, V. K.; Bulychev, B. M.; Golubeva, A. V. *Russ. J. Inorg. Chem*. **1983**, *28*, 1528.
(18) Hauback, B. C.; Brinks, H. W.; Jensen, C. M.; Murphy, K.; Maeland, A. J. *J. Alloys Compd*. **2003**, *358*, 142.
(19) Hauback, B. C.; Brinks, H. W.; Fjellvåg, H. *J. Alloys Compd*. **2002**, *346*, 184.
(20) Hauback, B. C.; Brinks, H. W.; Heyn, R. H.; Blom, R.; Fjellvåg, H. *J. Alloys Compd.* **2005**, *394*, 35.
(21) Fossdal, A.; Brinks, H. W.; Fichtner, M.; Hauback, B. C. *J. Alloys Compd*. **2005**, *387*, 47.
(22) Rönnebro, E.; Noréus, D.; Kadir, K.; Reiser, A.; Bogdanović, B. *J. Alloys Compd*. **2000**, *299*, 101.
(23) Brinks, H. W.; Hauback, B. C. *J. Alloys Compd*. **2003**, *354*, 143.
(24) Brinks, H. W.; Hauback, B. C.; Blanchard, D.; Jensen, C. M.; Fichtner, M.; Fjellvåg, H. *Adv. Mater. Energy Convers. II, TMS* **2004**, 197.
(25) Brinks, H. W.; Hauback, B. C.; Jensen, C. M.; Zidan, R. *J. Alloys Compd*. **2005**, *392*, 27.

(26) Garner, W. E.; Haycock, E. W. *Proc. R. Soc. (London)* **1952**, *A211*, 335.
(27) Ashby, E. C.; Kobetz, P. *Inorg. Chem.* **1966**, *5*, 1615.
(28) Dymova, T. N.; Bakum, S. I. *Russ. J. Inorg. Chem.* **1969**, *14*, 1683.
(29) Kuznetsov, V. A.; Golubeva, N. D.; Semenenko, K. N. *Russ. J. Inorg. Chem.* **1974**, *19*, 669.
(30) Dilts, J. A.; Ashby, E. C. *Inorg. Chem.* **1972**, *11*, 1230.
(31) Kiyobayashi, T.; Srinivasan, S. S.; Sun, D.; Jensen, C. M. *J. Phys. Chem. A* **2003**, *107*, 7671.
(32) Dymova, T. N.; Dergachev, Y. M.; Sokolov, V. A.; Grechanaya, N. A. *Dokl. Akad. Nauk SSSR.* **1975**, *224*, 591; *Engl. Ed.* **1976**, 556.
(33) Gross, K. J.; Guthrie, S.; Takara, S.; Thomas, G. *J. Alloys Compd.* **2000**, *297*, 270.
(34) Block, J.; Gray, A. P. *Inorg. Chem.* **1965**, *4* (3), 304.
(35) Chase, M. W.; Davies, C. A.; Downey, J. R.; Frurip, D. J.; McDonald, R. A.; Syverud, A. N. *JANAF Thermochem. Tab. (3rd ed.), J. Phys. Chem. Ref. Data, Suppl. 1.* **1985**, *14*, 1.
(36) Claudy, P.; Bonnetot, B.; Chahine, G.; Letoffe, J. M. *Thermochim. Acta* **1980**, *38*, 75.
(37) Bastide, J.-P.; Bonnetot, B.; Letoffe, J. M.; Claudy, P. *Mater. Res. Bull.* **1981**, *16*, 91.
(38) Morioka, H.; Kakizaki, K.; Chung, S.; Yamada, A. *J. Alloys Compd.* **2003**, *353*, 318.
(39) Clasen, H. *Angew. Chem.* **1961**, *73*, 322.
(40) Ashby, E. C.; Brendel, G. J.; Redman, H. E. *Inorg. Chem.* **1963**, *2*, 499.
(41) Wang, J.; Ebner, A. D.; Ritter, J. A. *J. Am. Chem. Soc.* **2006**, *128*, 5949.
(42) Wieberg, E.; Bauer, R.; Schmidt, M.; Uson, R. *Z. Naturforsch.* **1951**, *6b*, 393.
(43) Bogdanovic, B.; Schwickardi, M. *J. Serb. Chem. Soc.* **1989**, *54*, 579.
(44) German patent application 195 26 434.7, 1995.
(45) Jensen, C. M.; Zidan, R.; Mariels, N.; Hee, A.; Hagen, C. *Int. J. Hydrogen Energy* **1999**, *23*, 461.
(46) Zidan, R. A.; Takara, S.; Hee, A. G.; Jensen, C. M. *J. Alloys Compd.* **1999**, *285*, 119.
(47) Jensen, C. M.; Sun, D.; Murphy, K.; Wang, C.; Kumashiro, K.; Neimczura, W. *Proc. 2002 U.S. DOE Hydrogen and Fuel Cells Annual Program/Lab R&D Review*, May 6−10, 2002, Golden, CO.
(48) Bogdanović, B.; Brand, R. A.; Marjanovic, A.; Schwickardi, M.; Tölle, J. *J. Alloys Compd.* **2000**, *302*, 36.
(49) Zaluska, A.; Zaluski, L.; Ström-Olsen, J. O. *J. Alloys Compd.* **2000**, *298*, 125.
(50) Bogdanović, B.; Schwickardi, M. German Patent DE 19526434A1, 1995.
(51) Anton, D. L. *J. Alloys Compd.* **2003**, *356*, 400.
(52) Majzoub, E. H.; Gross, K. J. *J. Alloys Compd.* **2003**, *356−357*, 363.
(53) Srinivasan, S. S.; Brinks, H. W.; Hauback, B. C.; Sun, D.; Jensen, C. M. *J. Alloys Compd.* **2004**, *377*, 283.
(54) Gross, K. J.; Majzoub, E. H.; Spangler, S. W. *J. Alloys Compd.* **2003**, *356−357*, 423.
(55) Wang, P.; Jensen, C. M. *J. Phys. Chem. B* **2004**, *108*, 15827.
(56) Bogdanović, B.; Felderhoff, M.; Kaskel, S.; Pommerin, A.; Schlichte, K.; Schüth, F. *Adv. Mater.* **2003**, *15*, 1012−1015.
(57) Fichtner, M.; Fuhr, O.; Kircher, O.; Rothe, J. *Nanotechnology* **2003**, *14*, 778−785.
(58) Bogdanović, B.; Felderhoff, M.; Pommerin, A.; Schüth, F.; Spielkamp, N. *Adv. Mater.* **2006**, *18*, 1198.
(59) Wang, T.; Wang, J.; Ebner, A. D.; Ritter, J. A. *J. Alloys Compd.*, in press.
(60) Fossdal, A.; Brinks, H. W.; Fonneløp, J. E.; Hauback, B. C. *J. Alloys Compd.* **2005**, *397*, 135.
(61) Graetz, J.; Lee, Y.; Reilly, J. J.; Park, S.; Vogt, T. *Phys. Rev. B* **2005**, *71*, 184115.
(62) Balema, V. P.; Dennis, K. W.; Pecharsky, V. K. *Chem. Commun.* **2000**, 1665.
(63) Chen, J.; Kuriyama, N.; Xu, Q.; Takeshita, H. T.; Sakai, T. *J. Phys. Chem. B* **2001**, *105*, 11214.
(64) Blanchard, D.; Brinks, H. W.; Hauback, B. C.; Norby, P. *Mater. Sci. Eng. B* **2004**, *108* (1−2), 54.
(65) Sandrock, G.; Gross, K.; Thomas, G.; Jensen, C.; Meeker, D.; Takara, S. Submitted to *J. Alloys Compd.*
(66) Anton, D. L.; Mosher, M. A.; Opalka, S. M. *Proc. 2003 U.S. DOE Hydrogen Fuel Cells and Infrastrucutre Technologies Program Review*, May 19−22, 2003, Berkeley, CA.
(67) Srinivasan, S. S.; Brinks, H. W.; Hauback, B. C.; Sun, D.; Jensen, C. M. *J. Alloys Compd.* **2004**, *377*, 283.
(68) Chen, P.; Xiong, Z. T.; Luo, J. Z.; Lin, J. Y.; Tan, K. L. *Nature* **2002**, *420*, 303.
(69) Chen, P.; Xiong, Z. T.; Luo, J. Z.; Lin, J. Y.; Tan, K. L. *J. Phys. Chem. B* **2003**, *107*, 10967.
(70) Hu, Y. H.; Ruckenstein, E. *Ind. Eng. Chem. Res.* **2003**, *42*, 5135.
(71) Hu, Y. H.; Ruckenstein, E. *J. Phys. Chem. A* **2003**, *107*, 9737.
(72) Nakamori, Y.; Orimo, S. *Mat. Sci. Eng. B* **2004**, *108*, 48.
(73) Ichikawa, T.; Isobe, S.; Hanada, N.; Fujii, H. *J. Alloys Compd.* **2004**, *365*, 271.
(74) Nakamori, Y.; Orimo, S. *J. Alloys Compd.* **2004**, *370*, 271.
(75) Nakamori, Y.; Yamagishi, T.; Yokoyama, M.; Orimo, S. *J. Alloys Compd.* **2004**, *377*, L1.
(76) Ichikawa, T.; Hanada, N.; Isobe, S.; Leng, H. Y.; Fujii, H. *J. Phys. Chem. B* **2004**, *108*, 7887.
(77) Hu, Y. H.; Ruckenstein, E. *Ind. Eng. Chem. Res.* **2004**, *43*, 2464.
(78) Hu, Y. H.; Yu, Y. N.; Ruckenstein, E. *Ind. Eng. Chem. Res.* **2004**, *43*, 4174.
(79) Pinkerton, F. E. *J. Alloys Compd.* **2005**, *400*, 76.
(80) Meisner, G. P.; Pinkerton, F. E.; Balogh, M. S.; Kundrat, M. D. *J. Alloys Compd.* **2005**, *404*, 24.
(81) Isobe, S.; Ichikawa, T.; Hanada, N.; Leng, H. Y.; Fichtner, M.; Fuhr, O.; Fujii, H. *J. Alloys Compd.* **2005**, *404*, 439.
(82) Kojima, Y.; Kawai, Y. *J. Alloys Compd.* **2005**, *395*, 236.
(83) Hu, Y. H.; Ruckenstein, E. *Ind. Eng. Chem. Res.* **2005**, *44*, 1510.
(84) Hu, Y. H.; Yu, Y. N.; Ruckenstein, E. *Ind. Eng. Chem. Res.* **2005**, *44*, 4304.
(85) Yamane, H.; Kano, T.; Kamegawa, A.; Shibata, M.; Yamada, T.; Okada, M.; Shimada, M. *J. Alloys Compd.* **2005**, *402*, L1.
(86) Hu, Y. H.; Ruckenstein, E. *Ind. Eng. Chem. Res.* **2006**, *45* (182−186), 4993.
(87) Markmaitree, T.; Ren, R. M.; Shaw, L. L. *J. Phys. Chem. B* **2006**, *110*, 20710.
(88) Matsumoto, M.; Haga, T.; Kawai, Y.; Kojima, Y. *J. Alloys Compd.*, in press.
(89) Shaw, L. L.; Ren, R.; Markmaitree, T.; Osborn, W. *J. Alloys Compd.*, in press.
(90) Engbæk, J.; Nielsen, G.; Nielsen, J. H.; Chorkendorff, I. *Surf. Sci.* **2007**, *601*, 830.
(91) David, W. I. F.; Jones, M. O.; Gregory, D. H.; Jewell, C. M.; Johnson, S. R.; Walton, A. P.; Edwards, P. *J. Am. Chem. Soc.* **2007**, *129*, 1594.
(92) Bergstrom, F. W.; Fernelius, W. C. *Chem. Rev.* **1933**, *12*, 43.
(93) Gay-Lussac, J. L.; Thénard, L. J. *Ann. Phys.* **1809**, *32*, 1.
(94) Titherley, A. W. *J. Chem. Soc.* **1894**, *65*, 504.
(95) Dafert, F. W.; Miklauz, R. *Monatsh. Chem.* **1910**, *31*, 981.
(96) Ruff, O.; Georges, H. *Ber. Dtsch. Chem. Ges.* **1911**, *44*, 502.
(97) Nakamori, Y.; Kitahara, G.; Orimo, S. *J. Power Sources* **2004**, *138*, 309.
(98) Leng, H. Y.; Ichikawa, T.; Hino, S.; Hanada, N.; Isobe, S.; Fujii, H. *J. Phys. Chem. B* **2004**, *108*, 8763.
(99) Xiong, Z. T.; Chen, P.; Wu, G. T.; Lin, J. Y.; Tan, K. L. *J. Mater. Chem.* **2003**, *13*, 1676.
(100) Hino, S.; Ichikawa, T.; Leng, H. Y.; Fujii, H. *J. Alloys Compd.* **2005**, *398*, 62.
(101) Xiong, Z. T.; Wu, G. T.; Hu, H. J.; Chen, P. *Adv. Mater.* **2004**, *16*, 1522.
(102) Nakamori, Y.; Ninomiya, A.; Kitahara, G.; Aoki, M.; Noritake, T.; Miwa, K.; Kojima, Y.; Orimo, S. *J. Power Sources* **2006**, *155*, 447.
(103) Kojima, Y.; Matsumoto, M.; Kawai, Y.; Haga, T.; Ohba, N.; Miwa, K.; Towata, S.; Nakamori, Y.; Orimo, S. *J. Phys. Chem. B* **2006**, *110*, 9632.
(104) Xiong, Z. T.; Wu, G. T.; Hu, J. J.; Chen, P. *J. Power Sources* **2006**, *159*, 167.
(105) Lu, J.; Fang, Z. Z.; Sohn, H. Y. *J. Phys. Chem. B* **2006**, *110*, 14236.
(106) Xiong, Z. T.; Hu, J. J.; Wu, G. T.; Chen, P. *J. Alloys Compd.* **2005**, *395*, 209.
(107) Xiong, Z. T.; Wu, G. T.; Hu, J. J.; Chen, P. *J. Alloys Compd.* **2006**, *417*, 190.
(108) Hu, J. J.; Xiong, Z. T.; Wu, G. T.; Chen, P.; Murata, K.; Sakata, K. *J. Power Sources* **2006**, *159*, 116, 120.
(109) Liu, Y. F.; Hu, J. J.; Xiong, Z.; Wu, G. T.; Chen, P.; Murata, K.; Sakata, K. *J. Alloys Compd.* **2007**, *432*, 298.
(110) Liu, Y. F.; Liu, T.; Xiong, Z. T.; Hu, J. J.; Wu, G. T.; Chen, P.; Wee, A. T. S.; Yang, P.; Murata, K.; Sakata, K. *Eur. J. Inorg. Chem.* **2006**, 4368.
(111) Liu, Y. F.; Xiong, Z. T.; Hu, J. J.; Wu, G. T.; Chen, P.; Murata, K.; Sakata, K. *J. Power Sources* **2006**, *159*, 135.
(112) Kojima, Y.; Kawai, Y.; Ohba, N. *J. Power Sources* **2006**, *159*, 81.
(113) Orimo, S.; Nakamori, Y.; Kitahara, G.; Miwa, K.; Ohba, N.; Noritake, T.; Towata, S. *Appl. Phys. A* **2004**, *79*, 1765.
(114) Luo, W. F. *J. Alloys Compd.* **2004**, *381*, 284; **2004**, *385*, 316.
(115) Pinkerton, F. E.; Meisner, G. P.; Meyer, M. S.; Balogh, M. P.; Kundart, M. D. *J. Phys. Chem. B* **2005**, *109*, 6.
(116) Aoki, M.; Miwa, K.; Noritake, T.; Kitahara, G.; Nakamori, Y.; Orimo, S.; Towata, S. *Appl. Phys. A* **2005**, *80*, 1409.
(117) Noritake, T.; Aoki, M.; Towata, S.; Ninomiya, A.; Nakamori, Y.; Orimo, S. *Appl. Phys. A* **2006**, *83*, 277.
(118) Chater, P. A.; David, W. I. F.; Johnson, S. R.; Edwards, P. P.; Anderson, P. A. *Chem. Commun.* **2006**, *23*, 2439.

(119) Meisner, G. P.; Scullin, M. L.; Balogh, M. P.; Pinkerton, F. E.; Meyer, M. S. *J. Phys. Chem. B* **2006**, *110*, 4186.
(120) Pinkerton, F. E.; Meyer, M. S.; Meinster, G. P.; Balogh, M. P. *J. Phys. Chem. B* **2006**, *110*, 7967.
(121) Juza, V. R.; Opp, K. *Z. Anorg. Allg. Chem.* **1951**, *266*, 325.
(122) Jacob, H. V.; Juza, R. *Z. Anorg. Allg. Chem.* **1972**, *391*, 271.
(123) Grotjahn, D. B.; Sheridan, P. M.; Al Jihad, I.; Ziurys, L. M. *J. Am. Chem. Soc.* **2001**, *123*, 5489.
(124) Yang, J. B.; Zhou, X. D.; Cai, Q.; James, W. J.; Yelon, W. B. *Appl. Phys. Lett.* **2006**, *88*, 41914.
(125) Sørby, M. H.; Nakamura, Y.; Brinks, H. W.; Ichikawa, T.; Hino, S.; Fujii, H. B.; Hauback, C. *J. Alloys Compd.* **2007**, *428*, 297.
(126) Miwa, K.; Ohba, N.; Towata, S.; Nakamori, Y.; Orimo, S. *Phys. Rev. B* **2005**, *71*, 195109.
(127) Herbst, J. F.; Hector, L. G. *Phys. Rev. B* **2005**, *72*, 125120.
(128) Song, Y.; Guo, Z. X. *Phys. Rev. B* **2006**, *74*, 195120.
(129) Noritake, T.; Nozaki, H.; Aoki, M.; Towata, S.; Kitahara, G.; Nakamori, Y.; Orimo, S. *J. Alloys Compd.* **2005**, *393*, 264.
(130) Ohoyama, K.; Nakamori, Y.; Orimo, S.; Yamada, K. *J. Phys. Soc. Jpn.* **2005**, *74*, 483.
(131) Balogh, M. P.; Jones, C. Y.; Herbst, J. F.; Hector, L. G.; Kundrat, M. *J. Alloys Compd.* **2006**, *420*, 326.
(132) Janczyk, A.; Lichtenberger, D. L.; Ziurys, L. M. *J. Am. Chem. Soc.* **2006**, *128*, 1109.
(133) Mueller, T.; Ceder, G. *Phys. Rev. B* **2006**, *74*, 134104.
(134) Magyari-Kope, B.; Ozolins, V.; Wolverton, C. *Phys. Rev. B* **2006**, *73*, 220101.
(135) Zhang, C. J.; Dyer, M.; Alavi, A. *J. Phys. Chem. B* **2005**, *109*, 22089.
(136) Filinchuk, Y. E.; Yvon, K.; Meister, G. P.; Pinkerton, F. E.; Balogh, M. P. *Inorg. Chem.* **2006**, *45*, 1433.
(137) Herbst, J. F.; Hector, L. G. *Appl. Phys. Lett.* **2006**, *88*, 231904.
(138) Orimo, S.; Nakamori, Y.; Kitahara, G.; Miwa, K.; Ohba, N.; Towata, S.; Züttel, A. *J. Alloys Compd.* **2005**, *404*, 427.
(139) Jin, H. M.; Wu, P. *Appl. Phys. Lett.* **2005**, *87*, 181917.
(140) Zhang, C. J.; Alavi, A. *J. Phys. Chem. B* **2006**, *110*, 7139.
(141) Xiong, Z. T.; Hu, J. J.; Wu, G. T.; Chen, P.; Luo, W. F.; Gross, K.; Wang, J. *J. Alloys Compd.* **2005**, *398*, 235.
(142) Ichikawa, T.; Tokoyoda, K.; Leng, H. Y.; Fujii, H. *J. Alloys Compd.* **2005**, *400*, 245.
(143) Luo, W. F.; Ronnebro, E. *J. Alloys Compd.* **2005**, *404*−*406*, 392.
(144) Nakamori, Y.; Kitahara, G.; Miwa, K.; Ohba, N.; Noritake, T.; Towata, S.; Orimo, S. *J. Alloys Compd.* **2005**, *404*−*406*, 396.
(145) Leng, H. Y.; Ichikawa, T.; Isobe, S.; Hino, S.; Hanada, N.; Fujii, H. *J. Alloys Compd.* **2005**, *404*−*406*, 443.
(146) Luo, W. F.; Sickafoose, S. *J. Alloys Compd.* **2006**, *407*, 274.
(147) Leng, H. Y.; Ichikawa, T.; Hino, S.; Hanada, N.; Isobe, S.; Fujii, H. *J. Power Sources* **2006**, *156*, 166.
(148) Chen, Y.; Wu, C. Z.; Wang, P.; Chen, H. M. *Int. J. Hydrogen Energy* **2006**, *31*, 1236.
(149) Ichikawa, T.; Leng, H. Y.; Isobe, S.; Hanada, N.; Fujii, H. *J. Power Sources* **2006**, *159*, 126.
(150) Xiong, Z. T.; Wu, G. T.; Hu, J. J.; Chen, P.; Luo, W. F.; Wang, J. *J. Alloys Compd.* **2006**, *417*, 190.
(151) Yang, J.; Sudik, A.; Wolverton, C. *J. Alloys Compd.* **2007**, *430*, 334.
(152) Hu, Y. H.; Ruckenstein, E. *J. Phys. Chem. A* **2003**, *107*, 9737.
(153) Lu, J.; Fang, Z. G. Z.; Sohn, H. Y. *Inorg. Chem.* **2006**, *45*, 8749.
(154) Nakamori, Y.; Kitahara, G.; Miwa, K.; Towata, S.; Orimo, S. *Appl. Phys. A* **2005**, *80*, 1.
(155) Aoki, M.; Noritake, T.; Kitahara, G.; Nakamori, Y.; Towata, S.; Orimo, S. *J. Alloys Compd.* **2007**, *428*, 307.
(156) Nakamori, Y.; Kitahara, G.; Ninomiya, A.; Aoki, M.; Noritake, T.; Towata, S.; Orimo, S. *Mater. Trans.* **2005**, *46*, 2093.
(157) Aoki, M.; Noritake, T.; Nakamori, Y.; Towata, S.; Orimo, S. *J. Alloys Compd.*, in press.
(158) Alpati, S. V.; Johnson, J. K.; Sholl, D. S. *J. Phys. Chem. B* **2006**, *110*, 8769.
(159) Luo, W. F.; Stewart, K. *J. Alloys Compd.* **2007**, *440*, 357.
(160) Luo, W. F.; Wang, J.; Stewart, K.; Clift, M.; Gross, K. *J. Alloys Compd.*, in press.
(161) Noritake, T.; Aoki, M.; Towata, S.; Nakamori, Y.; Orimo, S. *Proc. MRS Meet. (Symp. Z: Hydrogen Storage Technol.)*, Nov. 27−30, 2006.
(162) Schlesinger, H. J.; Brown, H. C. *J. Am. Chem. Soc.* **1940**, *62*, 3429.
(163) Schlesinger, H. J.; Brown, H. C.; Hoekstra, H. R.; Rapp, L. R. *J. Am. Chem. Soc.* **1954**, *75*, 199.
(164) Goerrig, D. German Patent 1077644, 1958, F27373 IVa/12i.
(165) James, B. D.; Wallbridge, M. G. H. *Prog. Inorg. Chem.* **1970**, *11*, 99.
(166) Siegel, B.; Libowitz, G.; Mueller, W. M.; Blackledge, J. P. *Metal Hydrides*; Academic Press: New York, 1968.
(167) Nakamori, Y.; Li, H.; Miwa, K.; Towata, S.; Orimo, S. *Mater. Trans.* **2006**, *47* (8), 1898.
(168) Jeon, E.; Cho, Y. W. *J. Alloys Compd.* **2006**, *422*, 273.
(169) Köster, R. *Angew. Chem.* **1957**, *3*, 94.
(170) (a) Chłopek, K.; Frommen, Ch.; Léon, A.; Zabara, O.; Fichtner, M. *J. Mater. Chem.* **2007**, *17*, 3496. See also the recent topics on $Mg(BH_4)_2$. (b) Li, H. W.; Kikuchi, K.; Nakamori, Y.; Miwa, K.; Towata, S.; Orimo, S. *Scr. Mater.* **2007**, *57*, 679. (c) Cerny, R.; Filinchuk, Y.; Hagemann, H.; Yvon, K. *Angew. Chem., Int. Ed.* **2007**, *46*, 1. (d) Her, J. H.; Stephens, P. W.; Gao, Y.; Soloveichik, G. L.; Rijssenbeek, J.; Andrusb, M.; Zhao, J. C. *Acta Crystallogr.* **2007**, *B63*, 561. (e) Matsunaga, T.; Buchter, F.; Miwa, K.; Towata, S.; Orimo, S.; Züttel, A. *Renewable Energy*, in press.
(171) Long, L. H. *J. Inorg. Nucl. Chem.* **1979**, *32*, 1097.
(172) Fauroux, J. C.; Teichner, S. J. *Bull. Soc. Chim. Fr.* **1966**, *9*, 3014.
(173) Rao, B. K.; Jena, P.; Burkart, S.; Ganteför, G.; Seifert, G. *Phys. Rev. Let.* **2001**, *86* (4), 692.
(174) Wiberg, E.; Amberger, E. *Hydrides of the Elements of Main Groups I*−*IV*; Elsevier: Amsterdam, 1971.
(175) Marks, T. J.; Kolb, J. R. *Chem. Rev.* **1977**, *77* (2), 263.
(176) Lippard, S. J. *Progress in Inorganic Chemistry*; John Wiley & Sons: 1970; p 11.
(177) Harris, P. M.; Meibohm, E. P. *J. Am. Chem. Soc.* **1947**, *69*, 1231.
(178) Soulié, J.-P.; Renaudin, G.; Cerny, R.; Yvon, K. *J. Alloys Compd.* **2002**, *346*, 200.
(179) Züttel, A.; Rentsch, S.; Fischer, P.; Wenger, P.; Sudan, P.; Mauron, P.; Emmenegger, C. *J. Alloys Compd.* **2003**, *356*−*357*, 515.
(180) Lodziana, Z.; Vegge, T. *Phys. Rev. Lett.* **2004**, *93*, 145501.
(181) Miwa, K.; Ohba, N.; Towata, S.; Nakamori, Y.; Orimo, S. *Phys. Rev. B* **2004**, *69*, 245120.
(182) Johnston, H. L.; Hallet, N. C. *J. Am. Chem. Soc.* **1953**, *75*, 1467.
(183) Stockmeyer, W. H.; Stephenson, C. C. *J. Chem. Phys.* **1953**, *21*, 1311.
(184) Davis, R. L.; Kennard, C. L. *J. Solid State Chem.* **1985**, *59*, 393.
(185) Abrahams, S. C.; Kalnajs, J. *J. Chem. Phys.* **1954**, *22*, 434.
(186) Fischer, P.; Züttel, A. Order-Disorder Phase Transition in $Na[BD_4]$. *Trans. Tech. Publication Ltd. Proccedings of EPDIC-8*; 2002.
(187) Peterson, E. R. *Diss. Abstr.* **1965**, *25*, 5588.
(188) Ford, P. T.; Powell, H. M. *Acta Crystallogr.* **1954**, *7*, 604.
(189) Konoplev, V. N.; Bakulina, V. M. *Russ. Chem. Bull.* **1971**, *20* (1), 136.
(190) Fichtner, M.; Frommen, C.; Züttel, A. Synthesis and Properties of Magnesium Boranate. *Proc. Int. Symp. Met. Hydrogen Syst. Fund. Appl.*, Maui, Hawaii, U.S., 2006.
(191) Stockmayer, W. H.; Rice, D. W.; Stephenson, C. C. *J. Am. Chem. Soc.* **1955**, *77*, 1980.
(192) *Mellon's Comprehensive Treatise on Inorganic and Theoretical Chemistry, Vol. V Boron, Part B1: Boron-Hydrogen Compounds*; Longmans: 1981; p 354.
(193) Schrauzer, G. N. *Naturwissenschaften* **1955**, *42*, 438.
(194) Lippard, S. J.; Ucko, D. A. *Inorg. Chem.* **1968**, *7*, 1051.
(195) Lipscomb, W. N. *Boron Hydrides*; Benjamin: New York, 1963.
(196) Goebbert, D. J.; Hernandez, H.; Francisco, J. S.; Wenthold, P. G. *J. Am. Chem. Soc.* **2005**, *127* (33), 11684.
(197) Miwa, K.; Ohba, N.; Towata, S.; Nakamori, Y.; Orimo, S. *J. Alloys Compd.* **2005**, *404*−*406*, 140.
(198) Rittmeyer, P.; Wietelmann, U. *Ullmann's Encyclopedia of Industrial Chemistry, Hydrides, Ullmann's Encyclopedia of Industrial Chemistry V, A13: High-Performance Fibers to Imidazole and Derivatives*; p 199.
(199) Züttel, A.; Wenger, P.; Rentsch, S.; Sudan, P.; Mauron, P.; Emmenegger, C. *J. Power Sources* **2003**, *118*, 1.
(200) Vajeeston, P.; Ravindran, P.; Kjekshus, A.; Fjellvag, H. *Appl. Phys. Lett.* **2006**, *89*, 71906.
(201) Stasinevich, D. S.; Egorenko, G. A. *Russ. J. Inorg. Chem.* **1968**, *13* (3), 341.
(202) Davis, W. D.; Mason, L. S.; Stegeman, G. *J. Am. Chem. Soc.* **1949**, *71*, 2775.
(203) Züttel, A.; Borgschulte, A.; Orimo, S. *Scr. Mater.* **2007**, *56*, 823.
(204) Ohba, N.; Miwa, K.; Aoki, M.; Noritake, T.; Towata, S.; Nakamori, Y.; Orimo, S.; Züttel, A. *Phys. Rev. B* **2006**, *74*, 75110.
(205) Orimo, S.; Nakamori, Y.; Ohba, N.; Miwa, K.; Aoki, M.; Towata, S.; Züttel, A. *Appl. Phys. Lett.* **2006**, *89*, 21920.
(206) Soldate, A. M. *J. Am. Chem. Soc.* **1947**, *69*, 987.
(207) Gunn, S. R.; Green, L. G. *J. Chem. Phys.* **1962**, *36* (4), 1118 and (Erratum) **1962**, *37*, 2724.
(208) Kiran, B.; Kandalam, A. K.; Jena, P. *J. Chem. Phys.* **2006**, *124* (22), 224703.
(209) Barkhordarian, G.; Klassen, T.; Bormann, R. *J. Alloys Compd.* **2006**, *407*, 249.
(210) Orimo, S.; Nakamori, Y.; Züttel, A. *Mater. Sci. Eng. B* **2004**, *108* (1−2), 51.
(211) Nakamori, Y.; Miwa, K.; Ninomiya, A.; Li, H. W.; Ohba, N.; Towata, S.; Züttel, A.; Orimo, S. *Phys. Rev. B* **2006**, *74*, 45126.
(212) Frankcombe, T. J.; Kroes, G.-J.; Züttel, A. *Chem. Phys. Lett.* **2005**, *405*, 73.

(213) Nakamori, Y.; Li, H. W.; Kikuchi, K.; Aoki, M.; Miwa, K.; Towata, S.; Orimo, S. *J. Alloys Compd*., in press.
(214) Li, H. W.; Orimo, S.; Nakamori, Y.; Miwa, K.; Ohba, N.; Towata, S. *J. Alloys Compd*., in press.
(215) Fedneva, E. M.; Alpatova, V. L.; Mikheeva, V. I. *Russ. J. Inorg. Chem*. **1964**, *9* (6), 826.
(216) (a) Miwa, K.; Ohba, N.; Towata, S.; Nakmaori, Y.; Züttel, A.; Orimo, S. *J. Alloys Compd*., in press. (b) Nakamori, Y.; Li, H.-W.; Kikuchi, K.; Aoki, M.; Miwa, K.; Towata, S.; Orimo, S. *J. Alloys Compd.*, in press.
(217) Nakamori, Y.; Orimo, S.; Tsutaoka, T. *Appl. Phys. Lett*. **2006**, *88*, 112104.
(218) Matsuo, M.; Nakamori, Y.; Yamada, K.; Orimo, S.; Tsutaoka, T. *Appl. Phys. Lett*. **2007**, *90*, 232907.
(219) Grochala, W.; Edwards, P. P. *Chem. Rev.* **2004**, *104*, 1283.
(220) Arroyo y de Dompablo, M. E.; Ceder, G. *J. Alloys Compd*. **2004**, *364*, 6.
(221) Schüth, F.; Bogdaniović, B.; Felderhoff, M. *Chem. Commun*. **2004**, 2249.
(222) Seayad, A. M.; Antonelli, D. M. *Adv. Mater*. **2004**, *16*, 765.
(223) Orgaz, E.; Membrillo, A.; Castaneda, R.; Aburto, A. *J. Alloys Compd*. **2005**, *404*−*406*, 176.
(224) Yoshino, M.; Komiya, K.; Takahashi, Y.; Shinzato, Y.; Yukawa, H.; Morinaga, M. *J. Alloys Compd*. **2005**, *404*−*406*, 185.
(225) Fichtner, M. *Adv. Eng. Mater*. **2005**, *7*, 443.
(226) Dornheim, M.; Eigen, N.; Barkhordarian, G.; Klassen, T.; Bormann, R. *Adv. Eng. Mater*. **2006**, *8*, 377.
(227) Ross, D. K. *Vacuum* **2006**, *80*, 1084.
(228) Maj, Ł.; Grochala, W. *Adv. Funct. Mater*. **2006**, *16*, 2061.
(229) Fujii, H.; Ichikawa, T. *Physica B* **2006**, *383*, 45.
(230) Eberle, U.; Arnold, G.; von Helmolt, R. *J. Power Sources* **2006**, *154*, 456.
(231) Bogdanović, B.; Eberle, U.; Felderhoff, M.; Schüth, F. *Scr. Mater*. **2007**, *56*, 813.
(232) Chen, P.; Xiong, Z. T.; Wu, G. T.; Liu, Y. F.; Hu, J. J.; Luo, W. F. *Scr. Mater*. **2007**, *56*, 817.
(233) Vajo, J. J.; Olson, G. L. *Scr. Mater*. **2007**, *56*, 829.
(234) Graetz, J.; Reilly, J. J. *Scr. Mater*. **2007**, *56*, 835.
(235) Dornheim, M.; Doppiu, S.; Barkhordarian, G.; Boesenberg, U.; Klassen, T.; Gutfleisch, O.; Bormann, R. *Scr. Mater*. **2007**, *56*, 841.
(236) Eigen, N.; Keller, C.; Dornheim, M.; Klassen, T.; Bormann, R. *Scr. Mater*. **2007**, *56*, 847.
(237) Gomes, S.; Hagemann, H.; Yvon, K. *J. Alloys Compd.* **2002**, *346*, 206.
(238) Ge, Q. F. *J. Phys. Chem.* **2004**, *108*, 8682.
(239) Hagemann, H.; Gomes, S.; Renaudin, G.; Yvon, K. *J. Alloys Compd.* **2004**, *363*, 129.
(240) Renaudin, G.; Gomes, S.; Hagemann, H.; Keller, L.; Yvon, K. *J. Alloys Compd.* **2004**, *375*, 98.
(241) Moysés Araújo, C.; Li, S.; Ahuja, R.; Jena, P. *Phys. Rev. B* **2005**, *72*, 165101.
(242) Kumar, R. S.; Cornelius, A. L. *Appl. Phys. Lett.* **2005**, *87*, 261916.
(243) Vajeeston, P.; Ravindran, P.; Kjekshus, A.; Fjellvag, H. *J. Alloys Compd.* **2005**, *387*, 97.
(244) Varin, R. A.; Chiu, C. *J. Alloys Compd.* **2005**, *397*, 276.
(245) Bald, C. P.; Hereijgers, B. P. C.; Bitter, J. H.; de Jong, K. P. *Angew. Chem.* **2006**, *45*, 3501.
(246) Wang, J.; Ebner, A. D.; Ritter, J. A. *J. Am. Chem. Soc.* **2006**, *128*, 5949.
(247) Łodziana, Z.; Vegge, T. *Phys. Rev. Lett.* **2006**, *97*, 119602.
(248) Cho, Y. W.; Shim, J. H.; Lee, B. J. *CALPHAD: Comput. Coupling Phase Diagrams Thermochem.* **2006**, *30*, 65.
(249) Lee, G.; Lee, J. Y.; Kim, J. S. *Solution State Commun.* **2006**, *139*, 516.
(250) Du, A. J.; Smith, S. C.; Lu, G. Q. *Phys. Rev. B* **2006**, *74*, 193405.
(251) Hao, T.; Matsuo, M.; Nakamori, Y.; Orimo, S. *J. Alloys Compd.*, in press.
(252) Komiya, K.; Morisaku, N.; Shinzato, Y.; Ikeda, K.; Orimo, S.; Ohki, Y.; Tatsumi, K.; Yukawa, H.; Morinaga, M. *J. Alloys Compd*., in press.
(253) Matsunaga, T.; Buchter, F.; Mauron, P.; Bielman, M.; Nakamori, Y.; Orimo, S.; Ohba, N.; Miwa, K.; Towata, S.; Züttel, A. *J. Alloys Compd*., in press.
(254) (a) *SCI Finder Scholar*: "Hazardous Substances Data Bank" data are provided by the National Library of Medicine (U.S.). (b) *CRC Handbook of Chemistry and Physics*, 83rd ed.; CRC Press: Boca Raton, FL, 2002−2003. (c) Jacobs, H.; von Osten, E. *Z. Naturforsch. B-A J. Chem. Sci*. **1976**, 385. (d) Jacobs, H. *Z. Anorg. Allg. Chem*. **1976**, *427* (1), 8. (e) Løvvik, O. M.; Swang, O.; Opalka, S. M. *J. Mater. Res*. **2005**, *20*, 3199. (f) Løvvik, O. M.; Molin, P. N. *AIP Conf. Proc*. **2006**, *837*, 85.
(255) Balema, V. P.; Dennis, K. W.; Pecharsky, V. K. *Chem. Commun*. **2000**, 1665.
(256) Chen, J.; Kuriyama, N.; Xu, Q.; Takeshita, H. T.; Sakai, T. *J. Phys. Chem. B* **2001**, *105*, 11214.
(257) Kiyobayashi, T.; Srinivasan, S. S.; Sun, D.; Jensen, C. M. *J. Phys. Chem. A* **2003**, *107*, 7671.
(258) Au, M.; Jurgensen, A. *J. Phys. Chem. B* **2006**, *110*, 7062.
(259) Frankcombe, T. J.; Kroes, G. J. *Phys. Rev. B* **2006**, *73*, 174302.
(260) Vajo, J. J.; Skeith, S. L.; Mertens, F. *J. Phys. Chem. B* **2005**, *109*, 3719.
(261) Barhordarian, G.; Klassen, T.; Dornheim, M.; Bormann, R. R. *Solid State Commun*. **2006**, *139*, 516.
(262) Alapati, S. V.; Johnson, J. K.; Sholl, D. S. *J. Phys. Chem. B* **2006**, *110*, 8769.
(263) Kang, J. K.; Kim, S. Y.; Han, Y. S.; Muller, R. P.; Goddard, W. A. *Appl. Phys. Lett*. **2005**, *87*, 111904.
(264) Johnson, S. R.; Anderson, P. A.; Edwards, P. P.; Gameson, I.; Prendergast, J. W.; Al-Mamouri, M.; Book, D.; Harris, I. R.; Speight, J. D.; Walton, A. *Chem. Commun*. **2005**, 2823.
(265) Yu, X. B.; Grant, D. M.; Walker, G. S. *Chem. Commun*. **2006**, *37*, 3906.
(266) Miwa, K.; Aoki, M.; Noritake, T.; Ohba, N.; Nakamori, Y.; Towata, S.; Züttel, A.; Orimo, S. *Phys. Rev. B* **2006**, *74*, 155122.
(267) Jensen, C. M.; Gross, K. J. *Appl. Phys. A* **2001**, *72*, 213.
(268) Jacobs, H.; Juza, R. *Z. Anorg. Allg. Chem*. **1969**, *370*, 254.

CR0501846